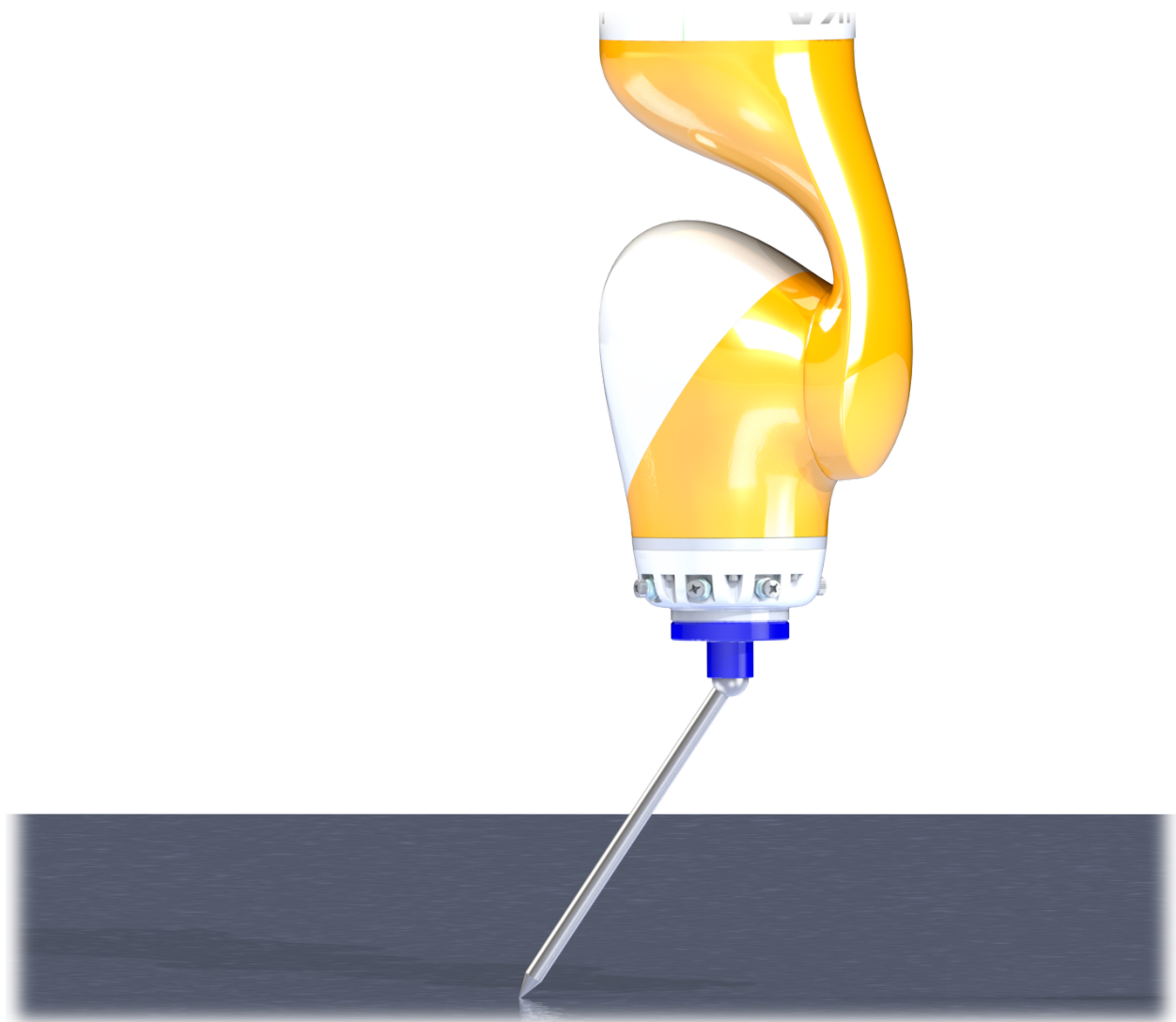




**CHALMERS**  
UNIVERSITY OF TECHNOLOGY

---



# **Robotic Constrained Manipulation with Adaptive Control**

Master's thesis in Systems, Control and Mechatronics

**MATHIAS FLECKENSTEIN**

---

Department of Signals and Systems  
CHALMERS UNIVERSITY OF TECHNOLOGY  
Gothenburg, Sweden 2016



MASTER'S THESIS 2016:NN

# Robotic Constrained Manipulation with Adaptive Control

MATHIAS FLECKENSTEIN



Department of Signals and Systems  
*Division of Automatic control, Automation and Mechatronics*  
Mechatronics  
CHALMERS UNIVERSITY OF TECHNOLOGY  
Gothenburg, Sweden 2016

Robotic Constrained Manipulation with Adaptive Control  
MATHIAS FLECKENSTEIN

© MATHIAS FLECKENSTEIN, 2016.

Supervisor: Assistant Professor Yiannis Karayiannidis, Signals and Systems  
Examiner: Assistant Professor Yiannis Karayiannidis, Signals and Systems

Master's Thesis 2016:NN  
Department of Signals and Systems  
Division of Automatic control, Automation and Mechatronics  
Mechatronics  
Chalmers University of Technology  
SE-412 96 Gothenburg

Cover: Manipulation of an unknown object with a Kuka LBR iiwa 14. The robot CAD file was downloaded from the Kuka Robotics GmbH homepage. The visualization was constructed and rendered in Solidworks 2015.

Typeset in L<sup>A</sup>T<sub>E</sub>X  
Printed by [Name of printing company]  
Gothenburg, Sweden 2016

Manipulation of an unknown, constrained object with the aid of a robot.

This master thesis project was initiated and conducted by Assistant Professor Yian-nis Karayiannidis, Chalmers University of Technology in cooperation with the University of Stuttgart within the Double Masters Degrees Program. The Department of Signals and Systems and the Institute for Control Engineering of Machine Tools and Manufacturing Units are the responsible institutions.

MATHIAS FLECKENSTEIN

Department of Signals and Systems  
Chalmers University of Technology

## Abstract

Robots employed in domestic settings need to manipulate and interact with objects whose motion is constrained by the environment. For instance, motion constraints can arise due to joints attaching an object to the environment. Commonly faced examples of this are doors and drawers. Additionally, constraints can be imposed by the contact between two objects, as for example, when an object is being manipulated on a supported surface. In this thesis we mainly consider the task of manipulating objects with pivoting dynamics. The manipulation task consists of rotating an unknown object around a pivot point by grasping the object in a way that allows relative rotation between the gripper and the object. In this case, two virtual revolute joints – one due to the pivot point on the surface and one due to the non-fixed grasp – impose kinematic constraints on the object. To perform the task we consider a velocity-controlled robot equipped with a force/torque sensor. The control law is designed as a velocity input that utilises a feed-forward term controlling the motion along the unconstrained direction and a PI-controller controlling the force along the constrained direction. Since the pivot point of the object is unknown, the kinematic parameters utilised in the controller, such as the direction of motion as well as kinematic parameters related to the object length and the rotation axis, are estimated on-line. To address the estimation problem, we consider Kalman-Bucy Filtering, Lyapunov-based adaptive laws and Immersion and Invariance (I&I)-based adaptive laws. A simulation model, based on Simulink<sup>®</sup>/SimMechanics<sup>™</sup> is developed in order to evaluate the performance of the adaptive controller in different scenarios. Considering both varying object lengths and sensor signals subject to different levels of measurement noise, we investigate the performance of the proposed estimators. Simulation results shows that the I&I-based adaptive controller has better convergence properties than the other methods.

Keywords: Adaptive control, Immersion and Invariance (I&I)-based adaptive law, Kalman-Bucy Filter, Lyapunov-based adaptive law parameter identification, state estimation, force/motion control, uncertain kinematics, constrained kinematics, robotic manipulation.



## Acknowledgements

I would like to thank my supervisor and examiner Yiannis Karayiannidis for his time and for giving me the opportunity to write this master thesis. His support was always constructive and helped me to reach this point.

Furthermore, I would like to thank the Baden-Württemberg Stiftung for the financial support with the Baden-Württemberg scholarship.

Last but not least, I would like to thank my family for their lovely support.

Mathias Fleckenstein, Gothenburg, June 2016



# Contents

<b>List of Figures</b>	<b>xi</b>
<b>List of Tables</b>	<b>xiii</b>
<b>Acronyms</b>	<b>xv</b>
<b>1 Introduction</b>	<b>1</b>
1.1 Main research question . . . . .	2
1.2 Related Work . . . . .	2
1.3 Methodology . . . . .	3
1.4 Thesis Organisation . . . . .	3
<b>2 Background</b>	<b>5</b>
2.1 Notation . . . . .	5
2.2 Adaptive Control . . . . .	6
2.2.1 Kalman-Bucy Filter . . . . .	7
2.2.2 Lyapunov-Based Adaptive Law . . . . .	8
2.2.3 Immersion and Invariance Based Adaptive Law . . . . .	9
<b>3 System and Problem Description</b>	<b>11</b>
3.1 Task Kinematics . . . . .	11
3.2 Robotic Kinematics . . . . .	15
3.3 Control Objective . . . . .	16
<b>4 Controller Design</b>	<b>19</b>
4.1 Control Law . . . . .	19
4.2 On-Line Estimator Design . . . . .	20
4.2.1 Kalman Filter with Known Rotation Axis . . . . .	21
4.2.2 Kalman Filter with Unknown Rotation Axis . . . . .	22
4.2.3 Lyapunov-Based Adaptive Law . . . . .	22
4.2.4 Adaptive Law Design via Immersion and Invariance . . . . .	24
<b>5 Simulation Model</b>	<b>29</b>
5.1 Object-orientated Physical Modelling . . . . .	29
5.2 Velocity Controller . . . . .	30
<b>6 Results</b>	<b>31</b>

6.1	Simulation Results . . . . .	31
6.1.1	Simulation Results for Varying Object Length . . . . .	34
6.1.2	Simulation Results with Varying Desired Velocity . . . . .	36
6.1.3	Simulation Results with Noise . . . . .	38
6.1.4	Simulation Results with Varying Initial Error Angle . . . . .	40
6.2	Discussion . . . . .	41
<b>7</b>	<b>Conclusion</b>	<b>43</b>
	<b>Bibliography</b>	<b>45</b>

# List of Figures

1.1	Object manipulation with pivoting dynamics. . . . .	1
2.1	Block diagram of a direct adaptive controller. . . . .	6
3.1	Coordinate system transformation of the frames <i>World</i> { $W$ }, <i>Base</i> { $B$ }, <i>Supporting Point</i> { $S$ } and <i>End-effector</i> { $E$ }. . . . .	11
3.2	Angle parametrisation. . . . .	13
3.3	Example object. . . . .	14
3.4	Block diagram of the total system, c.f. [9]. . . . .	17
5.1	Cut-out from the Simulink <sup>®</sup> model of the task kinematics. . . . .	30
6.1	Estimation response of proposed estimators for the standard param- eters, Table 6.3 . . . . .	33
6.2	Simulated force error of the wrist mounted force sensor. . . . .	33
6.3	Estimation response of proposed estimators for inverse object length $\kappa = 2\text{m}^{-1}$ . . . . .	34
6.4	Estimation response of proposed estimators for inverse object length $\kappa = 20\text{m}^{-1}$ . . . . .	35
6.5	Estimation force error response of proposed estimators. . . . .	36
6.6	Estimation response of proposed estimators for desired velocity $v_d^* =$ $0.1\frac{\text{m}}{\text{s}}$ . . . . .	37
6.7	Estimation force error response of proposed estimators for the desired velocity $v_d^* = 0.1\frac{\text{m}}{\text{s}}$ . . . . .	38
6.8	Estimation response of proposed estimators for force measurement signal subjected to noise with variance $\sigma^2 = 1 \cdot 10^{-6}\text{N}$ . . . . .	39
6.9	Estimation force error response of proposed estimators for force mea- surement signal subjected to noise with variance $\sigma^2 = 1 \cdot 10^{-6}\text{N}$ . . . . .	39
6.10	Estimation response of proposed estimators for initial estimation error of the motion direction $\psi(0) = 0.5\text{rad}$ . . . . .	40
6.11	Estimation force error response of proposed estimators for initial es- timation error of the motion direction $\psi(0) = 0.5\text{rad}$ . . . . .	41



# List of Tables

4.1	Overview of the Estimators. . . . .	27
6.1	Gains and parameters of the controllers and estimators. . . . .	31
6.2	Initial estimates. . . . .	32
6.3	Standard values of the parameters. . . . .	32
6.4	Values of the parameter with varying inverse object length simulation. . . . .	34
6.5	Values of the parameter with varying inverse object length simulation. . . . .	35
6.6	Values of the parameter with varying desired velocity. . . . .	37
6.7	Values of the parameter with measurement signal noise. . . . .	38
6.8	Initial estimates. . . . .	40



# Acronyms

**DOF** degrees of freedom. 15

**I&I** Immersion and Invariance. v, ix, 3, 5, 9, 24, 25, 27, 31–33, 35–38, 41, 43

**LLSME** Linear Least Minimum Mean Square Estimator. 7

**PI** Proportional-Integral. v, 2, 19, 25, 30, 31



# 1

## Introduction

The influence of service robotics has been increased over recent years [1]. An indicator for that is the growing trend towards using service robots not only for industrial purposes, but also for personal and domestic usage. One crucial requirement for a successful manipulation of a number of tasks is to control the interaction between the robot and its environment. The best way to quantify the interaction is to measure the interaction force at the end-effector, since high forces are undesirable in order to avoid damage to the structure of the robot and the manipulated environment. The environment can consist of surfaces or objects, which possesses static or dynamical properties. In both cases, the permissible trajectory of the end-effector is restricted by kinematic constraints.

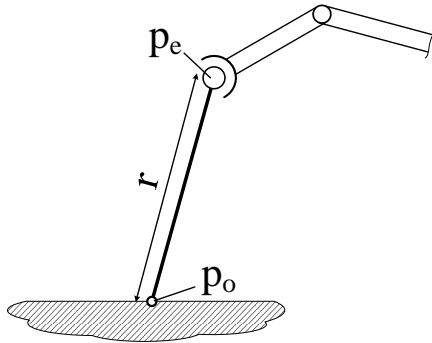


**Figure 1.1:** Object manipulation with pivoting dynamics.

There is a variety of possible interaction tasks. This thesis focuses on the manipulation of objects with pivoting dynamics, shown in Figure 1.1, since their manipulation enables to solve a wide range of problems within the service robotics field in domestic environment, for example opening doors. The scheme in Figure 1.1 shows an object, which possesses the aforementioned pivoting dynamics. More precisely, the object has one degree of freedom, so that it can only perform rotational motion around the supporting point on the surface. Assuming that the object and its posture is unknown, implies that the position of the pivoting point is unknown. Within this thesis a controller for a robot will be implemented to perform a manipulation task for unknown objects.

### 1.1 Main research question

The objective of this thesis is to identify the relevant constraints of pivoting manipulation (Figure 1.1), and use them in an adaptive controller in order to achieve the following manipulation task: rotating an unknown object around a pivot point by grasping the object in a way that allows relative rotation between the gripper and the object. In this case, two virtual revolute joints – one due to the pivot point on the surface and one due to the non-fixed grasp – impose kinematic constraints on the object. Since the object posture and its length is unknown, an adaptive controller has to be used to estimate these parameter uncertainties and to manipulate the object. The research work will be applicable in performing service robots for example to open unknown doors or turning a crank with a free knob.

### 1.2 Related Work

Since the topic of constrained manipulation is a common field of research in robotics, it is well-studied and lots of publications dealt with this topic. The books [2], [3] and [4] provide fundamental methods about modelling robot dynamics and kinematics in areas of unconstrained (non-contact) and constrained (interacted) manipulation. Especially, the kinematic formulations in these books are important for the description of the robot kinematics and its interaction with the environment. For this purpose, the interaction is modelled as geometric (kinematic) constraints. Furthermore, the aforementioned books give an overview of fundamental control techniques regarding motion and force control. These control structures are also applied to regulate the interaction of a robot with a dynamical environment assuming that the robot and the environment are modelled as a rigid body system. Article [5] presents the modelling of kinematic constraints and describes an example in which a crank with a free knob is turned. The manipulation of this crank possesses pivoting dynamics with a passive joint as is the case with the considered unknown object. Furthermore, article [6] analyses a camera navigation task on passive wrist-based robots and pivoting dynamics. Additionally, an adaptive PI-Cartesian position controller is presented for achieving the geometric modelled task of a laparoscopic assistant robot. Kinematic constraints are frequently used for modelling the manipulation task, since it simplifies the problem description. Article [7] analyses the manipulation with cooperating robots under uncertain kinematic parameters and presenting an adaptive controller which achieves parameter estimation during a desired object motion. The articles [8] and [9] cover the topic of opening doors under uncertainties with the aid of a velocity-controlled robot. The authors propose an adaptive controller which estimates the unconstrained motion direction and the inverse length of a door. The proposed adaptive laws - based on a Lyapunov function - are explained in this thesis and used for comparing the performance of different estimation methods, since a door possesses dynamics with pivoting characteristics. Moreover, in [8] the gripper of the robot posses a fixed grasp such that the relative rotation velocity between the end-effector and the door is zero. Article [9] additionally considers also a gripper with a non-fixed grasp which allows rotational velocity between the gripper and the

unknown object. Both proposed velocity controllers rely on force measurements and estimate the unconstrained motion direction, rotational axis and the relevant size of the door.

Kalman-Bucy Filtering is the second used estimator in this thesis to estimate the unconstrained motion direction and object length during the manipulation task. Since Kalman Filtering is a widespread method to observe, smooth or filter signals, there is a vast literature with theory and background. Therefore, this thesis focuses on books [10] and [11] which present the theoretical background of different Kalman Filters and describes their function. Moreover, these books show how to design a Kalman Filter for discrete or continuous systems.

The third used estimator is based on a relatively new design method for synthesising the adaptive laws. This framework is called Immersion and Invariance (I&I) and the book [12] and its related articles, [13], [14] and [4] provide the relevant background. The related literature cover not only the theory and methods synthesising I&I based adaptive controllers but also general used designing methods (e.g. Lyapunov). Moreover, [12] provides examples of the different synthesising methods and demonstrates the limits of the classical adaptive controllers.

## 1.3 Methodology

The research work is organised as follows:

- System modelling with constraints description
- Simulation environment development
- Adaptive controller design
- Scenario simulation
- Performance evaluation

First of all the dynamical system containing the unknown object and manipulator have to be analysed. For this purpose the system is assumed to be a rigid multibody system. The model building phase is an important step, since both, the simulation model and the control method will be based on it. Furthermore, the simulation model has to be implemented on a simulation platform, e.g. MATLAB<sup>®</sup>/Simulink<sup>®</sup>, to run simulated experiments. Subsequently, an adaptive controller must be designed to estimate on-line the object length and the unconstrained motion direction, which are the uncertain parameters of the manipulated system. Furthermore, the performance of the designed controller will be evaluated within the aforementioned simulation environment.

## 1.4 Thesis Organisation

This master thesis is organised with the following structure. First of all, Chapter 2 provides the general mathematical notation and background knowledge on adap-

tive control. Since the designed adaptive controller uses Kalman-Bucy Filtering, Lyapunov-based adaptive laws and I&I-based adaptive laws for estimating the unknown state and parameter, the background supplies the methods for synthesising these estimators. Chapter 3 describes the kinematic model of the unknown object and the robot. Additionally, this chapter formulates the control objective for a successful task execution. Chapter 4, aims at developing the simulation environment for testing the designed controller and synthesising the adaptive controller which includes the control law and the estimators. The performance of the developed adaptive controller is evaluated within different simulation scenarios in Chapter 6. Finally, conclusions are drawn in Chapter 7.

# 2

## Background

This chapter gives an overview of the used notation followed by relevant theory of adaptive control. Furthermore, Kalman-Bucy Filtering, Lyapunov-based and I&I-based adaptive controller are introduced for estimating parameters on-line.

### 2.1 Notation

The notation used in the thesis follows [15], [16] and [8] and is described in the following.

**Vectors and Matrices** Small bold letters denote vectors and capital bold letters denote matrices. Additionally,  $\mathbf{e}_i$ ,  $\hat{\mathbf{a}}$  and  $\tilde{\mathbf{a}}$  denote vectors with unit magnitude, estimates and the error between the actual and the desired/estimated vector, respectively. The vectors

$$\mathbf{a}(t) := \begin{bmatrix} a_x(t) & a_y(t) & a_z(t) \end{bmatrix}^\top \in \mathbb{R}^3,$$

$$\mathbf{b}(t) := \begin{bmatrix} b_x(t) & b_y(t) & b_z(t) \end{bmatrix}^\top \in \mathbb{R}^3,$$

are used in the following paragraphs to introduce further notation. Furthermore, the time argument is often dropped out for notation convenience.

**Projection Matrices** A projection matrix projecting vectors along vector  $\mathbf{a}$  is defined as

$$\mathbf{P}(\mathbf{a}) = \frac{\mathbf{a}\mathbf{a}^\top}{\|\mathbf{a}\|^2}$$

and possesses the property  $\mathbf{P}(\mathbf{a})^\top = \mathbf{P}(\mathbf{a})$ .

Matrix

$$\bar{\mathbf{P}}(\mathbf{a}) = \mathbf{I}_3 - \frac{\mathbf{a}\mathbf{a}^\top}{\|\mathbf{a}\|^2},$$

where  $\mathbf{I}_3 \in \mathbb{R}^3$  denotes the identity matrix, projects vectors on a space consisting of the orthogonal complements of vector  $\mathbf{a}$  and possesses the property  $\bar{\mathbf{P}}(\mathbf{a})^\top = \bar{\mathbf{P}}(\mathbf{a})$ .

**Skew-Symmetric Tensor** The skew-symmetric tensor

$$\mathbf{S}(\mathbf{a}) = \begin{bmatrix} 0 & -a_z & a_y \\ a_z & 0 & -a_x \\ -a_y & a_x & 0 \end{bmatrix}$$

can be used for representing a cross product operation as follows

$$\mathbf{a} \times \mathbf{b} = \mathbf{S}(\mathbf{a})\mathbf{b}.$$

Note that  $\mathbf{S}(\mathbf{a})\mathbf{b} = -\mathbf{S}(\mathbf{b})\mathbf{a}$ .

**Rotation Matrix** The orientation of a frame  $\{\mathbf{I}\}$  with respect to the frame  $\{\mathbf{J}\}$  is described by the rotation matrix  ${}^{\mathbf{I}}\mathbf{R}_{\mathbf{J}} \in \mathbb{R}^3$ . In case of  $\{\mathbf{I}\}$  or  $\{\mathbf{J}\}$  is identical to the robot base frame  $\{\mathbf{B}\}$ , the associated index will be omitted. A transformation from e.g.  $\{\mathbf{J}\}$  to the base frame can be calculated as following

$$\mathbf{a}_{\mathbf{I}} = \mathbf{R}_{\mathbf{J}} \mathbf{a}_{\mathbf{J}}.$$

Note that a rotation matrix is orthogonal and the inverse transformation can be written as  $\mathbf{R}^{-1} = \mathbf{R}^{\top}$ .

**Integral**  $\mathcal{I}(\mathbf{a}(t))$  denotes the element-wise time integration of the vector  $\mathbf{a}(t)$  and is defined as

$$\mathcal{I}(\mathbf{a}(t)) = \int_{t_0}^t \mathbf{a}(\tau) d\tau.$$

## 2.2 Adaptive Control

The performance of a conventional static control system is limited for dynamical processes, which have uncertain system parameters. These parameters could be, for example, unknown or time variant. Due to the dependency of the control law on the system parameters, the controller performance can be improved by an adaptive control structure which is shown in Figure 2.1.

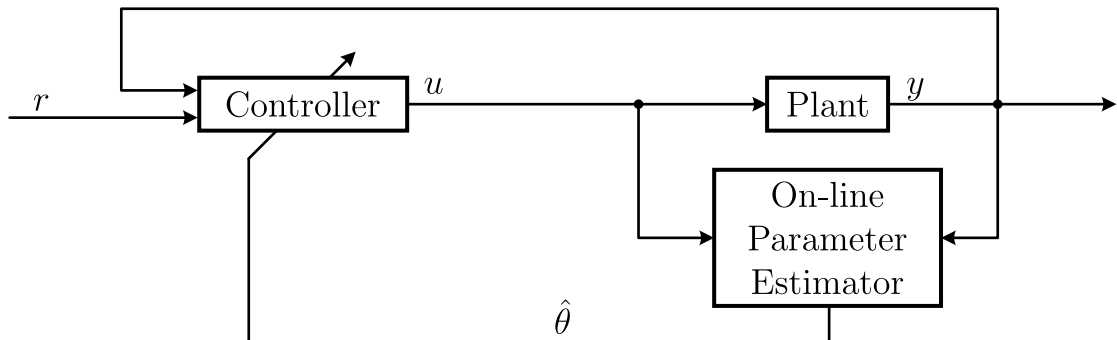


**Figure 2.1:** Block diagram of a direct adaptive controller.

Consider the dynamical system

$$\begin{aligned}\dot{\mathbf{x}}(t) &= \mathbf{f}(\mathbf{x}(t), \mathbf{u}(t), \boldsymbol{\theta}) \\ \mathbf{y}(t) &= \mathbf{h}(\mathbf{x}(t), \mathbf{u}(t), \boldsymbol{\theta})\end{aligned}\tag{2.1}$$

where  $\mathbf{x}(t) \in \mathbb{R}^n$  denotes the state vector,  $\mathbf{u}(t) \in \mathbb{R}^m$  the input vector,  $\boldsymbol{\theta} \in \mathbb{R}^q$  the parameter vector and  $\mathbf{y} \in \mathbb{R}^r$  the output vector. The plant in Figure 2.1 is represented by the dynamical system (2.1). Figure 2.1 shows also that the direct adaptive control structure consists of a parameter estimator and a controller block. The former provides the on-line estimates of the system parameters, which are the arrays of the estimated parameter vector  $\hat{\boldsymbol{\theta}}$ . Furthermore, the control law is designed for the known parameter case, cf. [17]. There are many different methods to deal with the on-line estimation. Since the performance of the adaptive controller highly depends on the estimation quality, it is necessary to use suitable estimation methods. The following sections introduce the estimation methods used in the present thesis.

### 2.2.1 Kalman-Bucy Filter

The Kalman filter is a Linear Least Minimum Mean Square Estimator (LLSME) for a linear system, since it minimizes a quadratic function of estimation error, cf. [11]. This type of filters is often used for filtering, prediction and smoothing of states, cf. [11]. The Kalman-Bucy filter is the continuous-time equivalent of the Kalman filter, which is formulated in discrete time. The following theory regarding the Kalman and Kalman-Bucy filter is based on the books [11] and [10].

Consider the dynamical system

$$\begin{aligned}\dot{\boldsymbol{\eta}}(t) &= \mathbf{F}(t)\boldsymbol{\eta}(t) + \mathbf{G}(t)\mathbf{w}(t) \\ \mathbf{z}(t) &= \mathbf{H}(t)\boldsymbol{\eta}(t) + \mathbf{v}(t)\end{aligned}\tag{2.2}$$

where  $\boldsymbol{\eta}(t) \in \mathbb{R}^l$  and  $\mathbf{z}(t) \in \mathbb{R}^k$  denotes the state vector of a random process and the measurement vector, respectively.  $\mathbf{F}(t) \in \mathbb{R}^{l \times l}$ ,  $\mathbf{G}(t) \in \mathbb{R}^{l \times w}$  and  $\mathbf{H}(t) \in \mathbb{R}^{k \times l}$  denote the time-varying dynamic coefficient, process noise coupling and measurement sensitivity matrix, respectively. Furthermore,  $\mathbf{w}(t) \in \mathbb{R}^w$  and  $\mathbf{v}(t) \in \mathbb{R}^k$  are the uncorrelated process and observation noise process, respectively. To ensure that the estimated states  $\hat{\boldsymbol{\eta}}(t)$  converge to their actual values, the system (2.2) must be observable. Furthermore,  $\mathbf{Q}(t) \in \mathbb{R}^{l \times l}$  and  $\mathbf{R}(t) \in \mathbb{R}^{k \times k}$ , which denotes the covariance matrices of  $\mathbf{w}(t)$  and  $\mathbf{v}(t)$ , are positive definite and are defined as

$$\begin{aligned}E\langle \mathbf{w}(t_1)\mathbf{w}^\top(t_2) \rangle &= \mathbf{Q}(t)\delta(t_2 - t_1), \\ E\langle \mathbf{v}(t_1)\mathbf{v}^\top(t_2) \rangle &= \mathbf{R}(t)\delta(t_2 - t_1),\end{aligned}$$

where  $E\langle \cdot \rangle$  and  $\delta(\cdot)$  stands for the expectancy operator and the Dirac delta function, respectively. The update equation  $\dot{\hat{\boldsymbol{\eta}}}(t)$  for the state estimation is expressed as

$$\dot{\hat{\boldsymbol{\eta}}}(t) = \mathbf{F}(t)\hat{\boldsymbol{\eta}}(t) + \mathbf{K}(t)(\mathbf{z}(t) - \mathbf{H}(t)\hat{\boldsymbol{\eta}}(t)),$$

where  $\mathbf{K}(t) \in \mathbb{R}^{l \times k}$  denotes the Kalman gain matrix and is defined as follows

$$\mathbf{K}(t) = \mathbf{P}(t)\mathbf{H}^\top(t)\mathbf{R}^{-1}(t). \quad (2.3)$$

The covariance matrix  $\mathbf{P}(t) \in \mathbb{R}^{l \times l}$  in (2.3) are calculated with the aid of the following Riccati differential equation

$$\begin{aligned} \dot{\mathbf{P}}(t) = & \mathbf{F}(t)\mathbf{P}(t) + \mathbf{P}(t)\mathbf{F}^\top(t) + \mathbf{G}(t)\mathbf{Q}(t)\mathbf{G}^\top(t) \\ & - \mathbf{P}(t)\mathbf{H}^\top(t)\mathbf{R}^{-1}(t)\mathbf{H}(t)\mathbf{P}(t). \end{aligned}$$

The initial conditions for these estimated states and the covariance matrix is defined as

$$\begin{aligned} \hat{\boldsymbol{\eta}}(0) &:= \hat{\boldsymbol{\eta}}_0 \\ \mathbf{P}(0) &:= \mathbf{P}_0. \end{aligned}$$

### 2.2.2 Lyapunov-Based Adaptive Law

Consider the dynamic system (2.1). As aforementioned, the adaptive control scheme includes the controller and the on-line parameter estimation component, which comprises the control law  $\mathbf{u}(\mathbf{x}, \boldsymbol{\theta})$  for the known parameters and the update law

$$\dot{\hat{\boldsymbol{\theta}}} = \mathbf{w}(\mathbf{x}, \hat{\boldsymbol{\theta}}).$$

Lyapunov functions are often used for analysing the stability of nonlinear systems. The direct Lyapunov method is also applicable for synthesising adaptive laws. In particular the problem of designing an adaptive controller is formulated as stability problem.

**Theorem 2.2.1** (Lyapunov Function).  *$V(\mathbf{x}, \boldsymbol{\theta}) \in \mathbb{R}$  is said to be a Lyapunov function of the system (2.1) if*

$$\begin{aligned} V(\mathbf{x}, \boldsymbol{\theta}) &> 0 && \text{in } \mathcal{D} \setminus \{0\} \\ \dot{V}(\mathbf{x}, \boldsymbol{\theta}) &\leq 0 && \text{in } \mathcal{D} \end{aligned} \quad (2.4)$$

*is satisfied, where  $\dot{V}(\mathbf{x}, \boldsymbol{\theta}) \in \mathbb{R}$  and  $\mathcal{D} = \{\mathbf{x} \subseteq \mathbb{R}^n, \boldsymbol{\theta} \subseteq \mathbb{R}^q\}$  denotes the derivative with respect to time of the Lyapunov function and the domain, respectively. Additionally,  $V(\mathbf{x}, \boldsymbol{\theta})$  has to be a continuously differentiable function, c.f. [18].*

For further reading, *Khalil* [18] provides more details on the Lyapunov theory.

**Assumption 2.1.** *There exists a Lyapunov function  $V(\mathbf{x}, \boldsymbol{\theta})$  so that the update law  $\dot{\hat{\boldsymbol{\theta}}}$  cancels the unknown parameter terms in  $\dot{V}(\mathbf{x}, \boldsymbol{\theta})$  and renders  $\dot{V}(\mathbf{x}, \boldsymbol{\theta})$  negative semi-definite, c.f. [12].*

The first step is to find a Lyapunov function candidate, which satisfies the requirement (2.4) of the Theorem 2.2.1. Furthermore, the update law  $\dot{\hat{\boldsymbol{\theta}}}$  has to be chosen in such a way so that  $\dot{V}(\mathbf{x}, \boldsymbol{\theta})$  is independent of the unknown parameters.

### 2.2.3 Immersion and Invariance Based Adaptive Law

The following background of the Immersion and Invariance (I&I) framework is based on the book [12] and its associated articles [13], [14]. I&I is a relatively new method for designing asymptotic stabilising controllers and adaptive laws for classes of uncertain nonlinear systems. Since I&I relies upon the notions of system immersion and manifold invariance, the knowledge of a suitable control Lyapunov function is not necessary. In this section the application of I&I for designing adaptive controllers is mainly described. The classical adaptive control design, as mentioned in Subsection 2.2.2, is often based on cancelling the  $\boldsymbol{\theta}$  dependent terms. The new framework of Immersion and Invariance (I&I) increases the robustness of the whole control system, since the cancellation of the parameter dependent terms in the Lyapunov-based adaptive law is a fragile operation which causes a manifold of equilibria, cf. [12].

Consider again the dynamical system (2.1). The basic idea of I&I is to immerse the given system into a system with predefined properties. Since  $\mathbf{f}(\cdot)$  is only partially known, the real parameters  $\boldsymbol{\theta}$  has to be estimated with the following augmented system

$$\begin{aligned}\dot{\mathbf{x}} &= \mathbf{f}(\mathbf{x}, \mathbf{u}, \boldsymbol{\theta}) \\ \dot{\hat{\boldsymbol{\theta}}} &= \mathbf{w}(\mathbf{x}, \hat{\boldsymbol{\theta}}),\end{aligned}$$

where  $(\mathbf{x}, \hat{\boldsymbol{\theta}}) \in \mathbb{R}^{n+q}$  defines the extended states. To apply successfully the Immersion and Invariance (I&I) methodology, the following Assumption must be satisfied.

**Assumption 2.2** (Adaptive stabilisability). *There exists a full-information control law  $\mathbf{u} = \mathbf{v}_{\text{cl}}(\mathbf{x}, \boldsymbol{\theta})$  (e.g. for the known parameter case), which stabilises the closed loop system*

$$\dot{\mathbf{x}} = \mathbf{f}(\mathbf{x}, \mathbf{v}_{\text{cl}}(\mathbf{x}, \boldsymbol{\theta}), \boldsymbol{\theta}),$$

so that all its trajectories are bounded.

**Definition 2.2.1.** *The system (2.1) will be classified as adaptive I&I stabilisable, if Assumption 2.2 is satisfied and if there exist a function  $\boldsymbol{\beta}(\cdot) \in \mathbb{R}^q$  and  $\mathbf{w}(\cdot) \in \mathbb{R}^q$ , so that the trajectories of the extended system*

$$\begin{aligned}\dot{\mathbf{x}} &= \mathbf{f}(\mathbf{x}, \mathbf{v}_{\text{cl}}(\mathbf{x}, \hat{\boldsymbol{\theta}} + \boldsymbol{\beta}(\mathbf{x})), \boldsymbol{\theta}) \\ \dot{\hat{\boldsymbol{\theta}}} &= \mathbf{w}(\mathbf{x}, \hat{\boldsymbol{\theta}})\end{aligned}\tag{2.5}$$

are bounded. Furthermore, the implicit manifold can be formulated as

$$\mathcal{M} = \{ \mathbf{x} \in \mathbb{R}^n, \hat{\boldsymbol{\theta}} \in \mathbb{R}^q : \hat{\boldsymbol{\theta}} - \boldsymbol{\theta} + \boldsymbol{\beta}(\mathbf{x}) = \mathbf{0} \}.$$

Additionally, the off-manifold coordinate  $\mathbf{z} := \hat{\boldsymbol{\theta}} - \boldsymbol{\theta} + \boldsymbol{\beta}(\mathbf{x})$ , with  $\mathbf{z} \in \mathbb{R}^q$ , has to satisfy

$$\lim_{t \rightarrow \infty} \mathbf{z}(t) = \lim_{t \rightarrow \infty} \hat{\boldsymbol{\theta}}(t) - \boldsymbol{\theta} + \boldsymbol{\beta}(\mathbf{x}(t)) = \mathbf{0},$$

so that the manifold  $\mathcal{M}$  is attractive, cf. [12].

## 2. Background

---

More precisely, Definition 2.2.1 means that the trajectories of  $\mathbf{x}$  and  $\hat{\boldsymbol{\theta}}$  asymptotically converges to the manifold  $\mathcal{M}$  and remains there. Additionally, the unknown parameter vector  $\theta$  is replaced by the expression  $\hat{\boldsymbol{\theta}} + \boldsymbol{\beta}(\mathbf{x})$ , such that the parameter estimation is not directly applied to the extended system (2.5).

# 3

## System and Problem Description

Section 3.1 elaborates on the manipulation task and the interaction between the manipulator, which is considered to be a robot, and the unknown object. After that the kinematics of the manipulator are analysed and it is defined how the control signal affects the end-effector velocity of the robot. Finally, Section 3.3 provides a detailed description of the control problem by introducing the control objective.

### 3.1 Task Kinematics

In this section, the kinematic constraints involved in the manipulation task are derived. The robot and the unknown object can be considered as a rigid body system in which the end-effector is connected with the object by a passive joint.

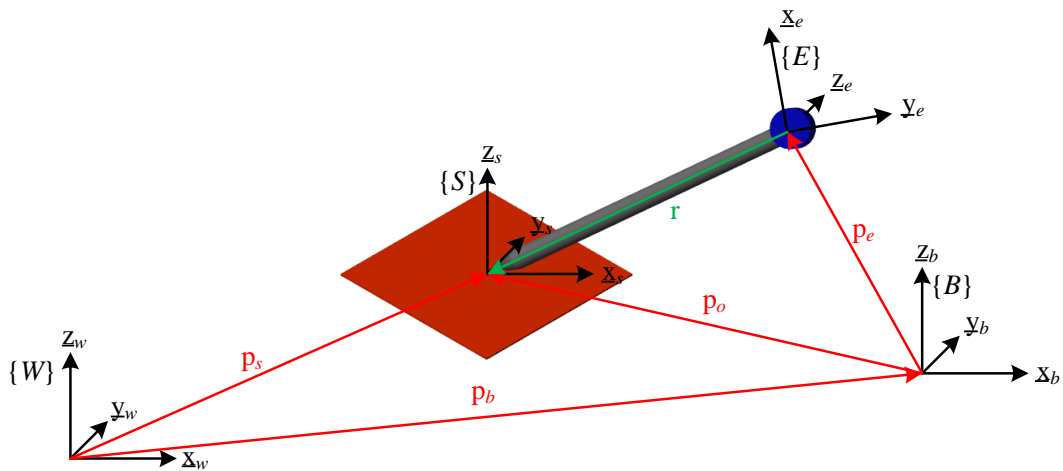


**Figure 3.1:** Coordinate system transformation of the frames *World* $\{W\}$ , *Base* $\{B\}$ , *Supporting Point* $\{S\}$  and *End-effector* $\{E\}$ .

Figure 3.1 shows an example for a possible constellation of the frames. The red vectors denote the translational relation between the used frames. The world frame  $\{W\}$  is a stationary reference coordinate system, which is the origin of a robot system. Furthermore, all other frames are related to  $\{W\}$ . The base coordinate system  $\{B\}$ , which is located at a robot's base, is the reference frame of the robot. Furthermore, the end-effector frame  $\{E\}$  represents the position and orientation of the end-effector, which is mounted at the Tool Centre Point (TCP) of the manipulator. The supporting point frame  $\{S\}$  is located at the contact point between the surface

### 3. System and Problem Description

---

and the unknown object and is therefore the centre of the rotational motion of the object. The unit vector  $\mathbf{z}_s \in \mathbb{R}^3$  is normal to the surface, while  $\mathbf{x}_s \in \mathbb{R}^3$ ,  $\mathbf{y}_s \in \mathbb{R}^3$  can be arbitrarily chosen.  $\{H\}$  denotes the handle frame which represents the position and orientation of the moveable end of the unknown object. The origin of the handle  $\{H\}$  and the end-effector frame  $\{E\}$  are located at the same position. This implies the following constraint for the position of the end-effector:

$$\mathbf{p}_e - \mathbf{p}_h \equiv 0,$$

where  $\mathbf{p}_e \in \mathbb{R}^3$  and  $\mathbf{p}_h \in \mathbb{R}^3$  denotes the position vector of the end-effector  $\{E\}$  and handle frame  $\{H\}$ , respectively.

**Assumption 3.1.** *There exists no relative translation between the end-effector and handle frame,*

$${}^h\dot{\mathbf{p}}_e \equiv 0.$$

**Assumption 3.2** (Planar Motion). *The motion of the unknown object is assumed to be planar. Therefore, the object can only afford one degree of freedom motion. Additionally, the rotation axis  $\mathbf{z}_h \in \mathbb{R}^3$  can be arbitrary and it is not necessary that  $\mathbf{z}_h \in \mathbb{R}^3$  and  $\mathbf{z}_b \in \mathbb{R}^3$  are parallel.*

Regarding Assumption 3.2, the orientation of  $\{H\}$  can be defined based on the rotational axis  $\mathbf{z}_h \in \mathbb{R}^3$  and the position of the unknown object and consequently on the constraints of the manipulation task. The vector  $\mathbf{y}_h \in \mathbb{R}^3$  is unit and points towards the origin of the supporting point frame  $\{S\}$ . Since Cartesian right-hand coordinate systems are used, the unconstrained motion direction  $\mathbf{x}_h \in \mathbb{R}^3$  can be formulated as

$$\mathbf{x}_h = \mathbf{S}(\mathbf{y}_h)\mathbf{z}_h.$$

Figure 3.2 depicts an alternative parametrisation of the handle frame vectors, which includes the rotation angle  $\varphi \in \mathbb{R}$  of the unknown object. The following vectors  $\mathbf{x}_h$ ,  $\mathbf{y}_h$  and  $\mathbf{z}_h$  describe the orientation of the handle frame  $\{H\}$  with respect to the base frame  $\{B\}$

$$\mathbf{x}_h = \mathbf{R}_s \begin{bmatrix} \cos \varphi \\ 0 \\ \sin \varphi \end{bmatrix}, \quad \mathbf{y}_h = \mathbf{R}_s \begin{bmatrix} -\sin \varphi \\ 0 \\ \cos \varphi \end{bmatrix}, \quad \mathbf{z}_h = \mathbf{R}_s \begin{bmatrix} 0 \\ 1 \\ 0 \end{bmatrix}, \quad (3.1)$$

where  $\mathbf{R}_s \in \mathbb{R}^3$  is the rotation matrix between the base  $\{B\}$  and surface frame  $\{S\}$ .

**Assumption 3.3** (Object Grasp). *The end-effector grasps the unknown object in a way that allows relative rotation between the end-effector and the object. Hence, the grasping point is considered as a passive joint.*

Due to Assumption 3.3, the orientation of  $\{H\}$  with respect to the end-effector

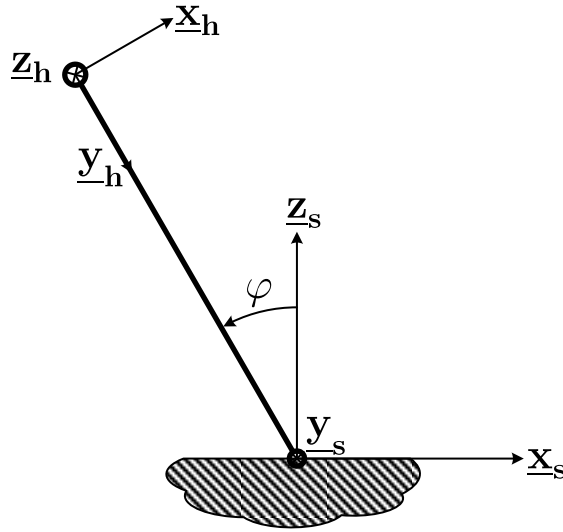


**Figure 3.2:** Angle parametrisation.

frame  $\{E\}$  and therefore the rotation matrix  ${}^e\mathbf{R}_h \in \mathbb{R}^3$  can be time-varying.

The radial vector  $\mathbf{r} \in \mathbb{R}^3$  represents the unknown object and connects the origins of the frames  $\{H\}$  and  $\{S\}$ . Since the origins of  $\{E\}$  and  $\{H\}$  are identical,  $\mathbf{r}$  connects also the origins of the frames  $\{E\}$  and  $\{S\}$ . Vector  $\mathbf{r}$  can be defined based on  $\mathbf{p}_o$  and  $\mathbf{p}_h$  or  $\mathbf{p}_e$  as follows:

$$\mathbf{r} := \mathbf{p}_o - \mathbf{p}_h = \mathbf{p}_o - \mathbf{p}_e \quad (3.2)$$

The radial vector  $\mathbf{r}$  is always parallel to  $\underline{\mathbf{y}}_h$ , therefore

$$\mathbf{r} = \frac{1}{\kappa} \underline{\mathbf{y}}_h. \quad (3.3)$$

is an alternative description for  $\mathbf{r}$ , where  $\kappa \in \mathbb{R}_0^+$  denotes the inverse length of the object line. Figure 3.3 depicts an example object including the object line, which always connects the end-effector and the contact point between the object and surface. Additionally,  $\kappa$  describes the curvature of the end-effector trajectory. By differentiating equation (3.2), the velocity  $\dot{\mathbf{r}}$  of the unknown object is as follows:

$$\begin{aligned} \dot{\mathbf{r}} &= \dot{\mathbf{p}}_o - \dot{\mathbf{p}}_h = \dot{\mathbf{R}}_h {}^h\mathbf{r} + \mathbf{R}_h {}^h\dot{\mathbf{r}} \\ &= \dot{\mathbf{R}}_h {}^h\mathbf{r} = \dot{\mathbf{R}}_h \mathbf{R}_h^T \mathbf{r} \\ &= \mathbf{S}(\boldsymbol{\omega}_h) \mathbf{r} = -\mathbf{S}(\mathbf{r}) \boldsymbol{\omega}_h, \end{aligned} \quad (3.4)$$

where  $\boldsymbol{\omega}_h \in \mathbb{R}^3$  denotes the rotational velocity of the handle frame  $\{H\}$ . The handle frame  $\{H\}$  is a body-fixed coordinate system of the unknown object, the rotational velocity of the unknown object  $\boldsymbol{\omega} \in \mathbb{R}^3$  can be expressed as

$$\boldsymbol{\omega} \equiv \boldsymbol{\omega}_h.$$

The rotational axis of the object and  $\underline{\mathbf{z}}_h$  are parallel, therefore an alternative expression of the rotational velocity vector is

$$\boldsymbol{\omega}_h = \omega \underline{\mathbf{z}}_h, \quad (3.5)$$

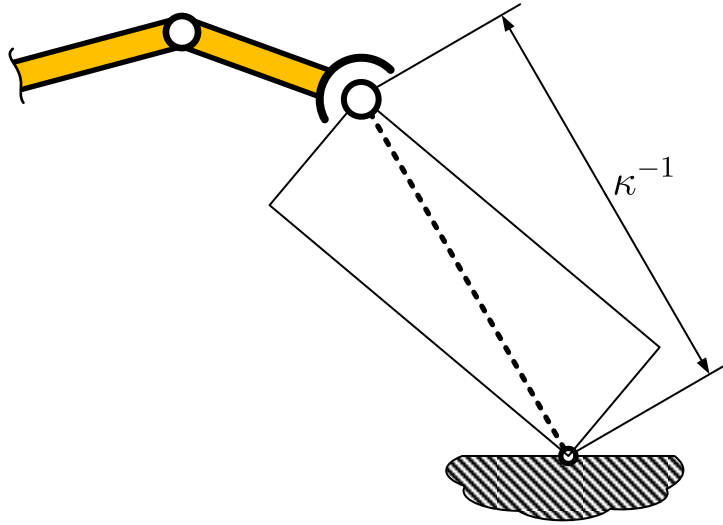


**Figure 3.3:** Example object.

where  $\omega$  denotes the magnitude of the rotational velocity. Since the end-effector  $\{E\}$  and handle frame  $\{H\}$  has the same origin, the end-effector velocity  $\mathbf{v} \in \mathbb{R}^3$  can be expressed with the aid of (3.4) as

$$\mathbf{v} = -\dot{\mathbf{r}} = \mathbf{S}(\mathbf{r})\boldsymbol{\omega}. \quad (3.6)$$

During this manipulation task, the dynamics of the interaction between the robot and its environment is restricted by kinematic constraints. In other words, the motion of the manipulated object is constrained, which causes forces, by moving along the constrained direction, cf. [2]. Since the end-effector trajectory is constrained by the object, the unconstrained motion direction is perpendicular to the radial vector  $\mathbf{r}$ . Because of the planar motion,  $\underline{\mathbf{x}}_{\mathbf{h}}$  is the motion direction by definition. From this it follows that the end-effector velocity  $\mathbf{v}$  can be parametrized as following

$$\mathbf{v} = v\underline{\mathbf{x}}_{\mathbf{h}}, \quad (3.7)$$

where  $v \in \mathbb{R}$  denotes the velocity magnitude of the end-effector.

Projecting the end-effector velocity  $\mathbf{v}$  along  $\underline{\mathbf{x}}_{\mathbf{h}}$  gives the scalar value

$$v = \underline{\mathbf{x}}_{\mathbf{h}}^{\top} \mathbf{v} \quad (3.8)$$

of the end-effector velocity. Furthermore, equation (3.7) implies that the constrained translational velocity of the end-effector is

$$\bar{\mathbf{P}}(\underline{\mathbf{x}}_{\mathbf{h}}) \mathbf{v} = 0.$$

Additionally, Equations (3.3),(3.5),(3.6) and (3.7) give the following relation between the translational and rotational velocities

$$v = \frac{\omega}{\kappa} \quad (3.9)$$

The differential kinematics of the unconstrained direction are given below:

$$\dot{\mathbf{x}}_{\mathbf{h}} = -\mathbf{S}(\mathbf{x}_{\mathbf{h}})\boldsymbol{\omega} \quad (3.10)$$

By substituting (3.5), (3.7) and (3.9) in Equation (3.10) gives

$$\dot{\mathbf{x}}_{\mathbf{h}} = -\mathbf{S}(\mathbf{v})\boldsymbol{\kappa}, \quad (3.11)$$

where  $\boldsymbol{\kappa} \in \mathbb{R}^3$  denotes the scaled direction vector  $\mathbf{z}_{\mathbf{h}}$  with length  $\kappa$ ,

$$\boldsymbol{\kappa} := \kappa\mathbf{z}_{\mathbf{h}}. \quad (3.12)$$

## 3.2 Robotic Kinematics

In order to manipulate an object whose motion is constrained by the environment as described in Section 3.1, it is necessary that the kinematic structure of the robot has sufficient number of degrees of freedom (DOF). In case of the pivoting manipulation task and considering that Assumption 3.3 is valid, 3-DOF are only enough if the angle of the trajectory of the unknown object is  $|\varphi(t) - \varphi(0)| \leq \pi$ . However, given that the initial position of the unknown object  $\varphi(0)$  and the rotation axis  $\mathbf{z}_{\mathbf{h}}$  are not known, a robot with 6 DOF is considered.

**Assumption 3.4** (Velocity-Controlled Robot). *In this thesis it is assumed that the end-effector motion of the manipulator can be velocity-controlled. The control signal*

$$\mathbf{u}_{\text{ref}} := \begin{bmatrix} \mathbf{v}_{\text{ref}} \\ \boldsymbol{\omega}_{\text{ref}} \end{bmatrix}$$

*consists of the translational and rotational control signal  $\mathbf{v}_{\text{ref}} \in \mathbb{R}^3$  and  $\boldsymbol{\omega}_{\text{ref}} \in \mathbb{R}^3$ , respectively.*<sup>1</sup>

Since the manipulation task is defined with respect to the end-effector, Assumption 3.4 simplifies the manipulation task formulation in terms of velocities instead of positions. Furthermore, the control signal  $\mathbf{u}_{\text{ref}}$  is specified in the task space and the robot is supposed to be controlled in the joint space. The control signal  $\mathbf{u}_{\text{ref}}$  is related to the joint velocities as follows:

$$\mathbf{u}_{\text{ref}} = \mathbf{J}(\mathbf{q})\dot{\mathbf{q}}, \quad (3.13)$$

where  $\dot{\mathbf{q}} \in \mathbb{R}^n$  denotes the joint velocities vector and  $\mathbf{J}(\mathbf{q}) \in \mathbb{R}^{n \times 6}$  the Jacobian matrix, which depends on the joint position vector  $\mathbf{q} \in \mathbb{R}^n$ . To reconstruct the joint velocities  $\dot{\mathbf{q}}$  from the control signal  $\mathbf{u}_{\text{ref}}$ , it is crucial to calculate the inverse transformation of Equation (3.13),

$$\dot{\mathbf{q}} = \mathbf{J}^+(\mathbf{q})\mathbf{u}_{\text{ref}}, \quad (3.14)$$

<sup>1</sup>Note that all control signals are expressed in the Base frame  $\{B\}$ .

where  $\mathbf{J}^+(\mathbf{q}) = \mathbf{J}(\mathbf{q})^\top [\mathbf{J}(\mathbf{q})\mathbf{J}(\mathbf{q})^\top]^{-1} \in \mathbb{R}^{6 \times n}$  denotes the pseudo inverse matrix of  $\mathbf{J}(\mathbf{q})$ , cf. [19]. Depending on the number of robot joints, the Jacobian matrix can be not square and therefore the real inverse matrix does not exist.

A manipulator can be mechanically represented as a kinematic chain of multi rigid bodies, cf. [2]. The kinematic structure of a robot is nearly always driven by an electrical actuator, which generates torque and thus accelerates the joints. Therefore, a motion controller is required for regulating the joint velocities  $\dot{\mathbf{q}}$  and thus the end-effector velocity  $\mathbf{v}$ .

**Assumption 3.5** (Ideal Motion Controller). *The inner motion control loop of the robot is sufficiently fast and includes a force and torque compensation, so that the joint velocity errors  $\dot{\tilde{\mathbf{q}}} \in \mathbb{R}^n$  between the desired and real value is negligible,*

$$\dot{\tilde{\mathbf{q}}} := \dot{\mathbf{q}} - \dot{\mathbf{q}}_d \approx \mathbf{0}.$$

Assumption 3.5 and Equation (3.14) implies that not only the error of the joint velocities  $\dot{\tilde{\mathbf{q}}}$  but also the error of the end-effector velocity:

$$\begin{aligned} \tilde{\mathbf{v}} &:= \mathbf{v} - \mathbf{v}_{\text{ref}} \approx \mathbf{0} \\ \tilde{\boldsymbol{\omega}} &:= \boldsymbol{\omega} - \boldsymbol{\omega}_{\text{ref}} \approx \mathbf{0} \end{aligned} \tag{3.15}$$

are negligible, where  $\tilde{\mathbf{v}} \in \mathbb{R}^3$  and  $\tilde{\boldsymbol{\omega}} \in \mathbb{R}^3$ . Furthermore, if Assumption 3.5 is valid, the object mass and inertia will have a strong influence on the force signal, which is generated by the wrist-mounted force sensors. Additionally, in order to reduce the risk of injuring humans in the domestic environment, the following Assumption has to be considered.

**Assumption 3.6** (Object Mass and Inertia). *The commanded velocity signals  $\mathbf{u}_{\text{ref}}$  of the end-effector and therefore, the unknown object is adequately low, such that the influence of object dynamics on the force measurement is negligible.*

### 3.3 Control Objective

Figure 3.4 shows the relevant parts and the interaction of the overall system. The following control objective is based on the article [9], that considers a similar manipulation task - opening a unknown door. First of all the interaction force  $\mathbf{f}_{\text{interaction}} \in \mathbb{R}^3$  between the unknown object and the robot has to be regulated. Consider the desired interaction force  $\mathbf{f}_d \in \mathbb{R}^3$ , one goal is to adjust the control signal  $\mathbf{u}_{\text{ref}}$ , so that the interaction force converges to the desired force  $\mathbf{f}_d$ . The interaction force objective can be satisfied by projecting the desired force along the constrained motion direction. The following equation describes the aforementioned first control objective,

$$\bar{\mathbf{P}}(\mathbf{x}_h)\mathbf{f} \rightarrow \bar{\mathbf{P}}(\mathbf{x}_h)\mathbf{f}_d.$$

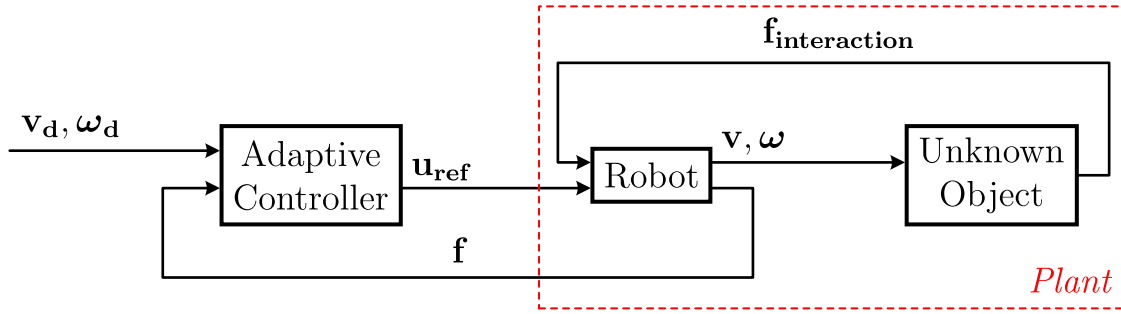


**Figure 3.4:** Block diagram of the total system, c.f. [9].

The second objective of the designed controller is to move the object, with a desired velocity  $v_d \in \mathbb{R}$ , on circular trajectory around the supporting point. Consider that the unconstrained motion direction is expressed in the object fixed handle frame  $\{H\}$ ,

$$\mathbf{v}_d = v_d \mathbf{x}_h, \quad (3.16)$$

where  $\mathbf{v}_d \in \mathbb{R}^3$  denotes the desired velocity vector of the end-effector. The second control objective is therefore,

$$\mathbf{v} \rightarrow \mathbf{v}_d$$

Due to the fact that the orientation and length of the object is not known, the orientation and its differential kinematics have to be estimated in the end-effector  $\{E\}$  or robot base frame  $\{B\}$ . Consider the vector  $\boldsymbol{\kappa}$  from Equation (3.12) which consists of the information of the rotation axis and the inverse length of the object and therefore combines two unknown parameters in one vector.

**Assumption 3.7** (Known Rotation Axis). *The rotation axis  $\mathbf{z}_h$  of the handle frame  $\{H\}$  is known.*

**Assumption 3.8** (Unknown Rotation Axis). *The rotation axis  $\mathbf{z}_h$  of the handle frame  $\{H\}$  is unknown.*

Depending which one of the following Assumption is satisfied, the control problem, especially the dimension of the estimation problem, changes.



# 4

## Controller Design

This chapter describes the control law and design of the different estimation algorithms. Since the overall performance of the manipulation task depends on the controller design, this part is an essential part of this master thesis.

### 4.1 Control Law

Let  $\hat{\mathbf{x}}_{\mathbf{h}} \in \mathbb{R}^3$  denote the estimate of the unconstrained motion direction. Since the robot is velocity controlled (Assumption 3.4), the output of the designed controller is the signal  $\mathbf{u}_{\text{ref}}$ . It is not necessary to control the rotational velocity of the end-effector, since the robot grasps the unknown object in a non-fixed way (Assumption 3.3). An additional rotational controller is only required for avoiding collisions between the unknown object and the end-effector or optimising the position of the robot joints. Therefore, the control signal  $\mathbf{u}_{\text{ref}}$  depends mainly on the translational velocity control signal  $\mathbf{v}_{\text{ref}}$ . As described in Section 3.3, the control law can be divided into two orthogonal terms. The first term is a feed-forward term controlling the motion along the unconstrained  $\mathbf{x}_{\mathbf{h}}$  and the second term is the term which controls the force along the constrained motion direction  $\bar{\mathbf{P}}(\mathbf{x}_{\mathbf{h}})$ . Consider the following control law

$$\mathbf{v}_{\text{ref}} = v_d \hat{\mathbf{x}}_{\mathbf{h}} - \bar{\mathbf{P}}(\hat{\mathbf{x}}_{\mathbf{h}}) \mathbf{v}_{\mathbf{f}} \quad (4.1)$$

which consists of the aforementioned orthogonal terms, c.f. [9]. Since  $\mathbf{x}_{\mathbf{h}}$  is not known, the control law (4.1) depends on the estimated unconstrained direction  $\hat{\mathbf{x}}_{\mathbf{h}}$ . Ideally,  $\hat{\mathbf{x}}_{\mathbf{h}}$  should have a unit magnitude, since it denotes a direction vector. If  $\|\hat{\mathbf{x}}_{\mathbf{h}}\| = 1$  the velocity of the end-effector  $v$  converge to the desired velocity  $v_d$ . The gain of the estimated motion direction  $v_d$  represents the desired velocity term of the control law, based on Equation (3.16). The second term of the control law (4.1), along the constrained direction, constructs the force controller. The vector  $\mathbf{v}_{\mathbf{f}} \in \mathbb{R}^3$  denotes the PI force feedback input with

$$\mathbf{v}_{\mathbf{f}} = \alpha_f \tilde{\mathbf{f}} + \beta_f \mathcal{I}[\bar{\mathbf{P}}(\hat{\mathbf{x}}_{\mathbf{h}}) \tilde{\mathbf{f}}], \quad (4.2)$$

where  $\alpha_f, \beta_f \in \mathbb{R}$  are positive control gains and

$$\tilde{\mathbf{f}} := \mathbf{f} - \mathbf{f}_d$$

denotes the force error, c.f. [9]. The force control term (4.2) compensates the kinematic uncertainties of the unknown object during the manipulation task. Additionally, term (4.2) also compensates partially the error between the estimated and real motion direction,  $\hat{\mathbf{x}}_{\mathbf{h}}$  and  $\mathbf{x}_{\mathbf{h}}$  respectively.

## 4.2 On-Line Estimator Design

As mentioned in Section 2.2, the direct adaptive control structure contains a controller and an on-line parameter estimation component. The following describes the details of designing different on-line parameter estimators, that estimate the unknown parameters  $\mathbf{x}_h$  and  $\boldsymbol{\kappa}$ . This parameter estimation adapts the control law in Subsection 4.1, since it uses these parameters for calculating the reference velocity of the end-effector.

In order to design an on-line estimator for the unknown parameters, the estimation errors have to be defined. In this regard,  $\tilde{\boldsymbol{\kappa}} \in \mathbb{R}^3$  denotes the error of the scaled rotation axis and is given by

$$\tilde{\boldsymbol{\kappa}}(t) = \hat{\boldsymbol{\kappa}}(t) - \boldsymbol{\kappa}. \quad (4.3)$$

Since  $\boldsymbol{\kappa}$  is constant, the derivative of estimation error of the inverse object length vector has the following form

$$\dot{\tilde{\boldsymbol{\kappa}}} = \dot{\hat{\boldsymbol{\kappa}}}. \quad (4.4)$$

The second estimation error is  $\psi(t) \in \mathbb{R}$  which defines the angular error of the motion direction. More precisely, it denotes the angle between the unknown  $\mathbf{x}_h$  and estimated unconstrained direction  $\hat{\mathbf{x}}_h$ . Since both directions are unit vectors, the inner product can be formulated as

$$\cos \psi(t) = \mathbf{x}_h^\top(t) \hat{\mathbf{x}}_h(t). \quad (4.5)$$

To get the relationship between the derivative of the error angle  $\psi(t)$  and the derivative of the estimated unknown direction, both sides of Equation (4.5) has to be differentiated as follows:

$$\begin{aligned} \frac{d}{dt}(\cos \psi(t)) &= \frac{d}{dt}(\mathbf{x}_h^\top \hat{\mathbf{x}}_h) \\ &= \dot{\mathbf{x}}_h^\top \hat{\mathbf{x}}_h + \mathbf{x}_h^\top \dot{\hat{\mathbf{x}}}_h \\ &= (-\mathbf{S}(\mathbf{v})\boldsymbol{\kappa})^\top \hat{\mathbf{x}}_h + \mathbf{x}_h^\top \dot{\hat{\mathbf{x}}}_h \\ &= -\mathbf{v}^\top \mathbf{S}(\boldsymbol{\kappa}) \hat{\mathbf{x}}_h + \mathbf{x}_h^\top \dot{\hat{\mathbf{x}}}_h \\ &= \mathbf{x}_h^\top (\dot{\hat{\mathbf{x}}}_h - v\mathbf{S}(\boldsymbol{\kappa})\hat{\mathbf{x}}_h) \\ \Leftrightarrow -\dot{\psi}(t) \sin \psi(t) &= \mathbf{x}_h^\top (\dot{\hat{\mathbf{x}}}_h - v\mathbf{S}(\boldsymbol{\kappa})\hat{\mathbf{x}}_h) \end{aligned} \quad (4.6)$$

The differentiation of (4.5) reveals that the error angle  $\psi(t)$  depends on the estimation rate and the object motion velocity, c.f. [9]. The velocity error  $\tilde{\mathbf{v}}$  can be expanded into one term along  $\hat{\mathbf{x}}_h$  and one term along its orthogonal complement space. Substituting the object velocity (3.7) and control law (4.1) in the velocity error formulation (3.15) leads to

$$\begin{aligned} \tilde{\mathbf{v}} &= v\mathbf{x}_h - v_d\hat{\mathbf{x}}_h + \bar{\mathbf{P}}(\mathbf{x}_h)\mathbf{v}_f \\ &= \mathbf{P}(\hat{\mathbf{x}}_h)\mathbf{v} + \bar{\mathbf{P}}(\hat{\mathbf{x}}_h)\mathbf{v} - v_d\hat{\mathbf{x}}_h + \bar{\mathbf{P}}(\mathbf{x}_h)\mathbf{v}_f \\ &= v \cos \psi \hat{\mathbf{x}}_h + \bar{\mathbf{P}}(\hat{\mathbf{x}}_h)\mathbf{v} - v_d\hat{\mathbf{x}}_h + \bar{\mathbf{P}}(\mathbf{x}_h)\mathbf{v}_f \\ &= \bar{\mathbf{P}}(\hat{\mathbf{x}}_h)(\mathbf{v} + \mathbf{v}_f) + (v \cos \psi - v_d) \hat{\mathbf{x}}_h. \end{aligned}$$

Assumption 3.5 and the resulting negligible velocity error implies the following closed-loop relations

$$\mathbf{P}(\hat{\mathbf{x}}_{\mathbf{h}}) \mathbf{v}_{\mathbf{f}} = -v \mathbf{P}(\hat{\mathbf{x}}_{\mathbf{h}}) \mathbf{x}_{\mathbf{h}} \quad (4.7)$$

$$v = \frac{v_d}{\cos \psi} \quad (4.8)$$

Taking the norm of the term along the complement space of  $\hat{\mathbf{x}}_{\mathbf{h}}$  gives

$$\|\mathbf{P}(\hat{\mathbf{x}}_{\mathbf{h}}) \mathbf{v}_{\mathbf{f}}\| = |v_d \tan \psi|. \quad (4.9)$$

For example 4.9 shows, how the estimation error  $\psi$  affects the force errors and the end-effector velocity error. Additionally, the closed-loop Equations (4.7), (4.8) and (4.9) give the evidence that the higher the unconstrained direction error  $\psi$  is, the higher the force on the object can be, c.f. [9].

### 4.2.1 Kalman Filter with Known Rotation Axis

If Assumption 3.7 (Known Rotation Axis) is satisfied, the linear parameter system will possess the following form

$$\begin{aligned} \dot{\boldsymbol{\theta}}(t) &= \mathbf{F}(t) \boldsymbol{\theta}(t) \\ \mathbf{z}(t) &= \mathbf{H}(t) \boldsymbol{\theta}(t), \end{aligned} \quad (4.10)$$

where  $\boldsymbol{\theta}(t) = [\mathbf{x}_{\mathbf{h}}^{\top}(t) \ \kappa]^{\top} \in \mathbb{R}^4$  is the parameter vector, which consists of the unknown parameters and  $\mathbf{F}(t) \in \mathbb{R}^{4 \times 4}$

$$\mathbf{F}(t) = \begin{bmatrix} \mathbf{0} & -\mathbf{S}(\mathbf{v}(t)) \mathbf{z}_{\mathbf{h}} \\ \mathbf{0} & 0 \end{bmatrix}$$

denotes the time-varying dynamic coefficient matrix. Its first row is based on the Equation (3.11) and since the object length is constant,  $\kappa$  is not varying. One possible measurement is the velocity of the end-effector, which is captured in the measurement vector  $\mathbf{z}(t) \in \mathbb{R}^3$ . From this it follows, that the measurement sensitivity matrix  $\mathbf{H}(t) \in \mathbb{R}^{3 \times 4}$  can be formulated as

$$\mathbf{H}(t) = [v(t) \mathbf{I}_3 \ \mathbf{0}].$$

Since the robot is velocity-controlled the matrices  $\mathbf{F}(t)$  and  $\mathbf{H}(t)$  can be expressed in terms of the reference velocity,

$$\begin{aligned} \mathbf{F}(t) &= \begin{bmatrix} \mathbf{0} & -\mathbf{S}(\mathbf{v}_{\text{ref}}(t)) \mathbf{z}_{\mathbf{h}} \\ \mathbf{0} & 0 \end{bmatrix} \\ \mathbf{H}(t) &= [v_{\text{ref}}(t) \mathbf{I}_3 \ \mathbf{0}]. \end{aligned}$$

Equation (3.8) and (3.15) shows that  $v_{\text{ref}}$  depends on the unknown state  $\mathbf{x}_{\mathbf{h}}$ . Using the expression

$$v_{\text{ref}}(t) = \|\mathbf{v}_{\text{ref}}(t)\| \operatorname{sgn}(\hat{\mathbf{x}}_{\mathbf{h}}^{\top}(t) \mathbf{v}_{\text{ref}}(t)) \quad (4.11)$$

it is possible to calculate  $v_{ref}$  without the knowledge of the motion direction for  $\hat{\mathbf{x}}_{\mathbf{h}}^\top \mathbf{x}_{\mathbf{h}} > 0$ , c.f. [9].

The update equation for the parameter estimation with known rotation axis is defined as

$$\dot{\hat{\boldsymbol{\theta}}} = \mathbf{F}(t)\hat{\boldsymbol{\theta}}(t) + \mathbf{K}(t) \left( \mathbf{z}(t) - \mathbf{H}(t)\hat{\boldsymbol{\theta}}(t) \right),$$

where  $\hat{\boldsymbol{\theta}}(t) = \left[ \hat{\mathbf{x}}_{\mathbf{h}}^\top(t) \quad \hat{\kappa}(t) \right]^\top$  denotes the estimated parameter vector. Furthermore, the Kalman gain matrix  $\mathbf{K}(t) \in \mathbb{R}^4$  can be calculated with the following equations,

$$\mathbf{K}(t) = \mathbf{P}(t)\mathbf{H}^\top(t)\mathbf{R}^{-1},$$

where  $\mathbf{R}(t) \in \mathbb{R}^{3 \times 3}$  denotes the covariance matrix of the measurement noise. The covariance matrix  $\mathbf{P}(t) \in \mathbb{R}^{4 \times 4}$  is calculated with the aid of the Riccati differential equation

$$\begin{aligned} \dot{\mathbf{P}}(t) &= \mathbf{F}(t)\mathbf{P}(t) + \mathbf{P}(t)\mathbf{F}^\top(t) + \mathbf{G}(t)\mathbf{Q}(t)\mathbf{G}^\top(t) \\ &\quad - \mathbf{P}(t)\mathbf{H}^\top(t)\mathbf{R}^{-1}(t)\mathbf{H}(t)\mathbf{P}(t), \end{aligned}$$

where  $\mathbf{Q} \in \mathbb{R}^3$  denotes the covariance matrix of the plant noise. The initial conditions for this Kalman filter are

$$\begin{aligned} \hat{\boldsymbol{\theta}}(0) &= \hat{\boldsymbol{\theta}}_0, \\ \mathbf{P}(0) &= \mathbf{P}_0. \end{aligned}$$

### 4.2.2 Kalman Filter with Unknown Rotation Axis

In case of unknown rotation axis, Assumption 3.8 is satisfied, the parameter system has the same form as (4.10). Consider the parameter vector  $\boldsymbol{\theta}(t) = \left[ \mathbf{x}_{\mathbf{h}}^\top(t) \quad \boldsymbol{\kappa}^\top \right] \in \mathbb{R}^6$ . The scaled rotation axis vector  $\boldsymbol{\kappa}$  consists of the inverted length  $\kappa$  and the rotation axis  $\mathbf{z}_{\mathbf{h}}$ , as mentioned in (3.12). Since the time-varying dynamic coefficient matrix  $\mathbf{F}(t) \in \mathbb{R}^{6 \times 6}$

$$\mathbf{F} = \begin{bmatrix} \mathbf{0} & -\mathbf{S}(\mathbf{v}(t)) \\ \mathbf{0} & \mathbf{0} \end{bmatrix}$$

does not include the information of the rotation axis  $\mathbf{z}_{\mathbf{h}}$ , the parameter system dimension increases to six. In this case the measurement sensitivity matrix  $\mathbf{H}(t) \in \mathbb{R}^{3 \times 6}$  has the following form,

$$\mathbf{H} = \begin{bmatrix} v(t)\mathbf{I}_3 & \mathbf{0} \end{bmatrix}.$$

The Kalman gain matrix  $\mathbf{K}(t) \in \mathbb{R}^{6 \times 3}$  and Riccati differential equation have the same form as in the known rotation axis case, only the dimension is different.

### 4.2.3 Lyapunov-Based Adaptive Law

The following design of the adaptive laws are based on the Article [9]. As described in the background, Section 2.2.2, the first step of the Lyapunov-based adaptive law design is to find an appropriate Lyapunov function candidate  $V$ , which depends on

the unknown motion direction  $\underline{\mathbf{x}}_h$  and the scaled rotation axis vector  $\boldsymbol{\kappa}$ . Consider the estimation error definition (4.5) of the unconstrained direction and (4.3) of the scaled object length vector.

Consider the Lyapunov function candidate

$$V = 1 - \cos \psi + \frac{1}{2} \tilde{\boldsymbol{\kappa}}^\top \boldsymbol{\Gamma}_\kappa \tilde{\boldsymbol{\kappa}}$$

which is positive definite for the domain  $\mathcal{D} = \{\psi \in \mathbb{R}, \tilde{\boldsymbol{\kappa}} \in \mathbb{R}^3 : |\psi| < \frac{\pi}{2}\}$ , cf. [9]. In order to satisfy Theorem 2.2.1 and to synthesise the adaptive laws, we calculate the derivative of the Lyapunov function  $\dot{V}(\psi, \tilde{\boldsymbol{\kappa}})$ :

$$\dot{V} = \dot{\psi} \sin \psi + \tilde{\boldsymbol{\kappa}}^\top \boldsymbol{\Gamma}_\kappa \dot{\tilde{\boldsymbol{\kappa}}},$$

where  $\boldsymbol{\Gamma}_\kappa \in \mathbb{R}^{3 \times 3}$  denotes a positive definite gain matrix. Substituting (4.3), (4.4) and (4.6) in  $\dot{V}$  leads to the following derivation:

$$\begin{aligned} \dot{V} &= -\underline{\mathbf{x}}_h^\top \left( \dot{\hat{\mathbf{x}}}_h - v \mathbf{S}(\hat{\boldsymbol{\kappa}} - \tilde{\boldsymbol{\kappa}}) \hat{\mathbf{x}}_h \right) + \tilde{\boldsymbol{\kappa}}^\top \boldsymbol{\Gamma}_\kappa \dot{\tilde{\boldsymbol{\kappa}}} \\ &= -\underline{\mathbf{x}}_h^\top \left( \dot{\hat{\mathbf{x}}}_h - v \mathbf{S}(\hat{\boldsymbol{\kappa}}) \hat{\mathbf{x}}_h + v \mathbf{S}(\tilde{\boldsymbol{\kappa}}) \hat{\mathbf{x}}_h \right) + \tilde{\boldsymbol{\kappa}}^\top \boldsymbol{\Gamma}_\kappa \dot{\tilde{\boldsymbol{\kappa}}} \\ &= -\underline{\mathbf{x}}_h^\top \left( \dot{\hat{\mathbf{x}}}_h + v \mathbf{S}(\hat{\mathbf{x}}_h) \hat{\boldsymbol{\kappa}} \right) - v \underline{\mathbf{x}}_h^\top \mathbf{S}(\tilde{\boldsymbol{\kappa}}) \hat{\mathbf{x}}_h + \tilde{\boldsymbol{\kappa}}^\top \boldsymbol{\Gamma}_\kappa \dot{\tilde{\boldsymbol{\kappa}}} \\ &= -\underline{\mathbf{x}}_h^\top \left( \dot{\hat{\mathbf{x}}}_h + v \mathbf{S}(\hat{\mathbf{x}}_h) \hat{\boldsymbol{\kappa}} \right) - v \tilde{\boldsymbol{\kappa}}^\top \mathbf{S}(\hat{\mathbf{x}}_h) \underline{\mathbf{x}}_h + \tilde{\boldsymbol{\kappa}}^\top \boldsymbol{\Gamma}_\kappa \dot{\tilde{\boldsymbol{\kappa}}} \\ &= -\underline{\mathbf{x}}_h^\top \left( \dot{\hat{\mathbf{x}}}_h + v \mathbf{S}(\hat{\mathbf{x}}_h) \hat{\boldsymbol{\kappa}} \right) - \tilde{\boldsymbol{\kappa}}^\top \left( v \mathbf{S}(\hat{\mathbf{x}}_h) \underline{\mathbf{x}}_h - \boldsymbol{\Gamma}_\kappa \dot{\tilde{\boldsymbol{\kappa}}} \right) \\ &= -\underline{\mathbf{x}}_h^\top \left( \dot{\hat{\mathbf{x}}}_h + v \mathbf{S}(\hat{\mathbf{x}}_h) \hat{\boldsymbol{\kappa}} \right) - \tilde{\boldsymbol{\kappa}}^\top \left( \mathbf{S}(\hat{\mathbf{x}}_h) \mathbf{v} - \boldsymbol{\Gamma}_\kappa \dot{\tilde{\boldsymbol{\kappa}}} \right) \end{aligned} \quad (4.12)$$

According to Theorem 2.2.1, the next step is to select the adaptive laws such that  $\dot{V}$  is negative semi-definite and the unknown parameters are cancelled. The article [9] proposes the following update law for  $\hat{\mathbf{x}}_h$

$$\dot{\hat{\mathbf{x}}}_h = -v_{\text{ref}} \mathbf{S}(\hat{\mathbf{x}}_h) \hat{\boldsymbol{\kappa}} - \gamma v_{\text{ref}} \bar{\mathbf{P}}(\hat{\mathbf{x}}_h) \mathbf{v}_f, \quad (4.13)$$

where  $\gamma \in \mathbb{R}^+$  is a positive constant control gain for tuning the update rate. Due to Assumption 3.4 (Velocity-Controlled Robot) is valid, the scalar velocity of the end-effector  $v$  can be substituted by the scalar reference velocity  $v_{\text{ref}}$ . The first term update law (4.13) cancels the unknown parameters in (4.12) for sufficient high  $\gamma$ . Since the unconstrained direction  $\underline{\mathbf{x}}_h$  is time varying, the second term is necessary to ensure the convergence of  $\hat{\mathbf{x}}_h$  to the unknown motion direction  $\underline{\mathbf{x}}_h$ . The update law for  $\hat{\mathbf{x}}_h$  depends on the estimation of the estimated scaled rotation axis  $\hat{\boldsymbol{\kappa}}$ , which can be on-line estimated by the update law

$$\dot{\hat{\boldsymbol{\kappa}}} = \boldsymbol{\Gamma}_\kappa \mathbf{S}(\hat{\mathbf{x}}_h) \mathbf{v}_{\text{ref}}. \quad (4.14)$$

Projecting (4.7) along the motion direction  $\underline{\mathbf{x}}_h$  and substituting (4.5) yields

$$\begin{aligned} \underline{\mathbf{x}}_h^\top \bar{\mathbf{P}}(\hat{\mathbf{x}}_h) \mathbf{v}_f &= -v \underline{\mathbf{x}}_h^\top \bar{\mathbf{P}}(\hat{\mathbf{x}}_h) \underline{\mathbf{x}}_h \\ &= -v \underline{\mathbf{x}}_h^\top \left( \mathbf{I}_3 - \hat{\mathbf{x}}_h \hat{\mathbf{x}}_h^\top \right) \underline{\mathbf{x}}_h \\ &= -v(1 - \cos^2 \psi) = -v \sin^2 \psi. \end{aligned} \quad (4.15)$$

Due to the manipulator is velocity-controlled,  $v$  can be substituted by  $v_{ref}$  in (4.15). Substituting the update laws (4.13) and (4.14) shows that  $\dot{V}$  is negative semi-definite due to the cancelled terms and equation (4.15). Therefore,  $V$  satisfies the Theorem 2.2.1. Additionally,  $v_{ref}$  can be calculated in the same way as in (4.11).

The control law (4.1) suggests that the estimated motion direction vector  $\hat{\mathbf{x}}_h$  must be unit in order to achieve the desired control objective. The update law  $\dot{\hat{\mathbf{x}}}_h$  ensures that the norm of the unconstrained direction vector  $\hat{\mathbf{x}}_h(t)$  is invariant. Projecting  $\dot{\hat{\mathbf{x}}}_h$  along the  $\hat{\mathbf{x}}_h$  yields

$$\begin{aligned} \hat{\mathbf{x}}_h^\top \dot{\hat{\mathbf{x}}}_h &= -v_{ref} \hat{\mathbf{x}}_h^\top \mathbf{S}(\hat{\mathbf{x}}_h) \hat{\boldsymbol{\kappa}} - \gamma v_{ref} \hat{\mathbf{x}}_h^\top \bar{\mathbf{P}}(\hat{\mathbf{x}}_h) \mathbf{v}_f \\ \Leftrightarrow \frac{d}{dt} \left( \frac{1}{2} \|\hat{\mathbf{x}}_h\|^2 \right) &= -v_{ref} \hat{\boldsymbol{\kappa}}^\top \mathbf{S}(\hat{\mathbf{x}}_h) \hat{\mathbf{x}}_h - \gamma v_{ref} \hat{\mathbf{x}}_h^\top \left( \mathbf{I}_3 - \hat{\mathbf{x}}_h \hat{\mathbf{x}}_h^\top \right) \mathbf{v}_f \\ &= -v_{ref} \hat{\boldsymbol{\kappa}}^\top \mathbf{S}(\hat{\mathbf{x}}_h) \hat{\mathbf{x}}_h - \gamma v_{ref} \left( \hat{\mathbf{x}}_h^\top - \hat{\mathbf{x}}_h^\top \hat{\mathbf{x}}_h \hat{\mathbf{x}}_h^\top \right) \mathbf{v}_f = 0 \end{aligned}$$

From this it follows that  $\|\hat{\mathbf{x}}_h(0)\| = \|\hat{\mathbf{x}}_h(t)\|$ ,  $\forall t \geq 0$  and therefore, if the initial value of the estimated motion direction is  $\|\hat{\mathbf{x}}_h(0)\| = 1$  the magnitude will be unit at all time.

The article [9] provides more details on the stability analysis and the convergence of the estimated parameters.

#### 4.2.4 Adaptive Law Design via Immersion and Invariance

Considering the alternative parametrisation (3.1) of the handle frame  $\{H\}$  which depends on the scalar parameter  $\varphi$  and Assumption 3.7 is satisfied. Therefore, the estimation problem consists of two scalar parameters, the angle  $\varphi$  and the inverted object length  $\kappa$ . Additionally, for this case the second column of the rotation matrix  $\mathbf{R}_s$  is known and the rotation axis  $\mathbf{z}_h$  can be calculated. Since the following problem formulation is based on the angle error  $\psi$  and its dynamics  $\dot{\psi}$ , the rotational velocity of the object can be parametrised as

$$\dot{\varphi} = -v\kappa.$$

Furthermore, the aforementioned angle error  $\psi$  is defined in this case as

$$\psi := \hat{\varphi} - \varphi. \quad (4.16)$$

The derivative of (4.16) yields to the first-order differential equation, which is part of the augmented system

$$\begin{aligned} \dot{\psi} &= \dot{\hat{\varphi}} + v\kappa \\ \dot{\hat{\kappa}} &= w, \end{aligned} \quad (4.17)$$

where  $w \in \mathbb{R}$  denotes the update law and define in the extended space  $(\psi, \hat{\kappa}) \in \mathbb{R}^2$  the implicit manifold

$$\mathcal{M} = \{\psi \in \mathbb{R}, \hat{\kappa} \in \mathbb{R} : \hat{\kappa} - \kappa + \beta(\psi) = 0\}.$$

The dynamics of the augmented system (4.17) is restricted by the manifold  $\mathcal{M} \in \mathbb{R}$ . The invariance property of the manifold  $\mathcal{M}$  is described by the equation

$$\dot{\psi} = \dot{\hat{\varphi}} + v(\hat{\kappa} + \beta(\psi)).$$

The update law for  $\hat{\varphi}$  can be analogously designed for the known rotation axis with the angle parametrisation case as for the unknown rotation axis (4.13). In particular the update law is proposed as follows:

$$\dot{\hat{\varphi}} = -\gamma v_d v_f - v(\hat{\kappa} + \beta(\psi)), \quad (4.18)$$

where  $\gamma \in \mathbb{R}^+$  denotes the update rate gain. Furthermore,  $v_f$  denotes the scalar expression of the PI-force controller of the control law (4.1) and is defined as

$$v_f = \hat{\mathbf{y}}_{\mathbf{h}}^\top \mathbf{v}_f,$$

where  $\hat{\mathbf{y}}_{\mathbf{h}}$  is the estimated constrained direction (3.1). The next step of the I&I method is to select an update law for  $\hat{\kappa}$  which renders the manifold  $\mathcal{M}$  invariant. Consider the off-manifold  $z$  is given by

$$z := \hat{\kappa} - \kappa + \beta(\psi). \quad (4.19)$$

The following off-manifold dynamics  $\dot{z}$ , which is given by the time derivative of (4.19), must be asymptotic stable.

$$\begin{aligned} \dot{z} &= \dot{\hat{\kappa}} + \frac{\partial \beta(\psi)}{\partial \psi} \dot{\psi} \\ &= \dot{\hat{\kappa}} + \frac{\partial \beta(\psi)}{\partial \psi} [\dot{\hat{\varphi}} + v(\hat{\kappa} + \beta(\psi) - z)] \end{aligned} \quad (4.20)$$

In the next step the update law  $\dot{\hat{\kappa}}$  has to be chosen in such a way so that the manifold  $\mathcal{M}$  is invariant:

$$\dot{\hat{\kappa}} = -\frac{\partial \beta(\psi)}{\partial \psi} [\dot{\hat{\varphi}} + v(\hat{\kappa} + \beta(\psi))] \quad (4.21)$$

Substituting the update law for  $\hat{\kappa}$  (4.21) in the off-manifold dynamics (4.20) yields

$$\dot{z} = -\frac{\partial \beta(\psi)}{\partial \psi} z. \quad (4.22)$$

Consider the Lyapunov function candidate  $V$  in order to analyse the stability properties of the off-manifold dynamics (4.22) by the direct Lyapunov method.

$$V = \frac{1}{2} z^2 \quad (4.23)$$

The Lyapunov function candidate  $V$  in (4.23) is positive definite for all  $z \in \mathbb{R} \setminus \{0\}$ .

$$\dot{V}(z) = z\dot{z} = -\frac{\partial \beta(\theta)}{\partial \theta} z^2 \quad (4.24)$$

The selection of the function  $\beta(\psi)$  must consist of known components, since it appears in the update law for  $\hat{\varphi}$ . Proposing the function

$$\beta(\psi) = \gamma_\beta v_f,$$

where  $\gamma_\beta \in \mathbb{R}^+$  denotes a positive update rate gain. For further calculations the relations of the velocities (4.8), (4.9) have to be transformed in the known rotation axis case:

$$\begin{aligned} v &= v_d \frac{1}{\cos \psi} \\ v_f &= v_d \tan \psi \end{aligned}$$

From this it follows,  $\beta(\psi)$  and  $\frac{\partial \beta(\psi)}{\partial \psi}$  can be expressed in terms of  $\psi$ . Consider the  $\beta(\psi)$  function and its partial derivative  $\frac{\partial \beta(\psi)}{\partial \psi}$ :

$$\begin{aligned} \beta(\psi) &= \gamma_\beta v_d \tan \psi \\ \frac{\partial \beta(\psi)}{\partial \psi} &= \gamma_\beta v_d (1 + \tan^2 \psi) = \gamma_\beta v_d \left(1 + \frac{v_f^2}{v_d^2}\right) \end{aligned} \quad (4.25)$$

The function  $\beta(\psi)$  must be calculable with known values in order to apply this function to the update laws for the estimated object angle  $\hat{\varphi}$  and inverse object length  $\hat{\kappa}$ . Furthermore, substituting (4.25) in the time derivative of the Lyapunov function candidate (4.24) leads to

$$\dot{V}(z) = -\gamma_\beta v_d (1 + \tan^2 \psi) z^2$$

Given that  $v_d$  is chosen positive, the derivative of the Lyapunov function  $\dot{V}$  is negative definite and therefore the off-manifold dynamics are asymptotically stable with the equilibrium at  $z^* = 0$ , if  $\psi \in \mathcal{D}$ .

In order to obtain the final update law  $\dot{\hat{\varphi}}$ ,  $\beta(\psi)$  has to be substituted in Equation (4.18). The end-effector velocity  $v$  can be expressed in terms of the controlled end-effector velocity  $v_{\text{ref}}$ , since the manipulator is velocity-controlled (Assumption 3.4). This leads to the update law for  $\hat{\varphi}$ ,

$$\dot{\hat{\varphi}} = -\gamma v_d v_f - v_{\text{ref}} (\hat{\kappa} + \gamma_\beta v_f).$$

Furthermore, substituting Equation (4.18) and (4.25) in the update law for  $\hat{\kappa}$  (4.21) leads to

$$\dot{\hat{\kappa}} = \gamma \gamma_\beta v_f (v_d^2 + v_f^2).$$

The aforementioned estimators in this subsection have different properties. The following Table gives an overview of the properties and in what cases they could be applied:

---

<b>Estimation</b>	Kalman-Bucy Filter	Lyapunov-Based	I&I-Based
<b>Unconstrained Motion Direction</b>	✓	✓	✓
<b>Object Line</b>	✓	✓	✓
<b>Rotation Axis</b>	✓	✓	

**Table 4.1:** Overview of the Estimators.

Table 4.1 shows that the I&I-based estimator is only applicable for objects with known rotation axis.



# 5

## Simulation Model

In order to evaluate the performance of the designed adaptive controller, it is necessary to create a testing platform. This could be in this case a simulation model or a physical experiment. It is advisable to indicate the generality of the controller within a simulation model, since the tests of different simulation scenarios can be implemented in a short time. Additionally, the risk of damaging the experiment hardware can be reduced by testing the approach first in simulation. Since a simulation model is often an approximation of a real experiment setup, it is recommended to evaluate the performance of the adaptive controller in further experiments. In the following sections the used modelling method of the mechanical system and end-effector actuation is introduced.

### 5.1 Object-orientated Physical Modelling

As Albert Einstein said: "Everything should be made as simple as possible, but not simpler." This axiom could be applied for the simulation model which should be as simple as possible. In order to depict all relevant dynamics the simulation model should also be as close to the reality as necessary. Since the task kinematics in Section 3.1 is described by the constraints and the object inertia is assumed to be negligible (Assumption 3.6), it is reasonable to utilise a software platform for object-orientated physical modelling. With this modelling method it is not necessary to identify all dynamical equations of the system. The simulation environment SimMechanics™ Second Generation is used for modelling the mechanical structure of the systems, which is included in the SimScape™ toolbox. The considered rigid body system can be modelled by using blocks representing body elements, joints, frames and sensors in Simulink®, cf. [20].

Figure 5.1 depicts the modelling of the task kinematic which consists of the interaction dynamics of the unknown object and the surface. This object-orientated physical model contains body elements and joints which are linked by physical connections. As described in Assumption 3.2 the unknown object can rotate around the pivoting point on the surface. This constraint is represented by a revolute joint which also measures the angle, angular velocity and force between the unknown object and the surface. The passive joint, which is shown in Figure 5.1, represents the loose grasp of the unknown object by the robot end-effector. An additional advantage to use SimMechanics™ is that this toolbox provides an included animation framework. This animation gives users a visual feedback of the simulation and shows the

## 5. Simulation Model

simulation results without any additional implementation.

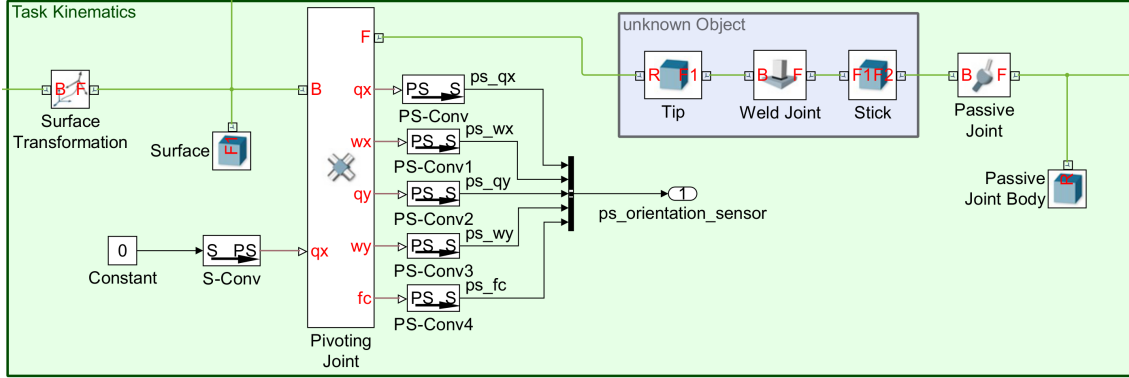


**Figure 5.1:** Cut-out from the Simulink<sup>®</sup> model of the task kinematics.

## 5.2 Velocity Controller

During the manipulation task, the robot end-effector must be able to move the object with a desired velocity. Since the SimMechanics<sup>™</sup> toolbox does not support velocity commanded actuation, the end-effector is actuated by forces. Calculating the desired forces with feed forward terms cause errors for objects with different geometries or masses, therefore a velocity PI-controller is applied to regulate the force  $\mathbf{f}_e \in \mathbb{R}^3$  on the end-effector. This PI-controller has the following form

$$\mathbf{f}_e = \alpha_v \tilde{\mathbf{v}}_e + \beta_v \mathcal{I} [\tilde{\mathbf{v}}_e],$$

where  $\alpha_v, \beta_v \in \mathbb{R}$  are positive controller gains and

$$\tilde{\mathbf{v}}_e := \mathbf{v}_{\text{ref}} - \mathbf{v}_e$$

denotes the velocity error of the end-effector between the controlled velocity  $\mathbf{v}_{\text{ref}}$  and the end-effector velocity  $\mathbf{v}_e \in \mathbb{R}^3$ .

# 6

## Results

This chapter contains the development of the simulation scenarios, in order to evaluate the performance of the designed estimators Kalman-Bucy Filtering with unknown rotation axis, Lyapunov-based adaptive laws and Immersion and Invariance-based adaptive laws. Furthermore, different scenarios are presented for the purpose to make inferences regarding the robustness of the adaptive controller. The simulation results base on the simulation model in Chapter 5.

### 6.1 Simulation Results

The following scenarios cover different object lengths, different desired velocities along the motion direction and the impact of the noise in the force sensor signal  $\mathbf{f}$ . With the aid of these scenarios, it is possible to demonstrate the robustness of the different estimation methods and reveal their strengths and weaknesses.

	Parameter	Value
<b>Velocity controller</b>	$\alpha_v$	25
	$\beta_v$	2
<b>Force Controller</b>	$\alpha_f$	$5 \cdot 10^{-2}$
	$\beta_f$	$5 \cdot 10^{-3}$
<b>Kalman-Bucy Filter</b>	$\mathbf{P}(0)$	$1 \cdot 10^5 \mathbf{I}_6$
	$\mathbf{R}$	$1 \cdot 10^{-4} \mathbf{I}_3$
	$\mathbf{Q}$	$1 \cdot 10^{-5}$
	$\mathbf{G}$	$[1 \ 1 \ 1 \ 1 \ 1 \ 1]^\top$
<b>Lyapunov</b>	$\gamma$	$2 \cdot 10^4$
	$\mathbf{\Gamma}_\kappa$	$2 \cdot 10^4 \mathbf{I}_3$
<b>I&amp;I</b>	$\gamma$	$5 \cdot 10^3$
	$\gamma_\beta$	$1 \cdot 10^4$

**Table 6.1:** Gains and parameters of the controllers and estimators.

The chosen parameters of the velocity PI-controller in the simulation model and the force PI-controller in the control law are displayed in Table 6.1 and are same for every scenario. Additionally, the initial values for the inverse object length and the motion direction offset are presented in the following Table.

Parameter	Initial Value	Unit
$\hat{\kappa}(0)$	7	$\text{m}^{-1}$
$\psi(0)$	0.2	rad

**Table 6.2:** Initial estimates.

All scenarios are tested with the same update rate gains or in case of Kalman-Bucy Filtering, Kalman parameters. In order to reduce the effect of velocity steps at the start, the following smooth trajectory of the desired velocity  $v_d(t)$  is used for the scenario simulations, cf. [9]:

$$v_d(t) = v_d^* (1 - e^{-10t}),$$

where  $v_d(t)$  denotes the first order low pass filtered desired velocity for steps and  $v_d^* \in \mathbb{R}$  denotes the end value. This has the advantage that jerk is reduced during the manipulation task, because of avoiding sharp initial transients. Additionally, the desired force  $f_d = 0$  is chosen for every scenario.

Parameter	Value	Unit
$\kappa$	5	$\text{m}^{-1}$
$v_d^*$	0.05	$\frac{\text{m}}{\text{s}}$

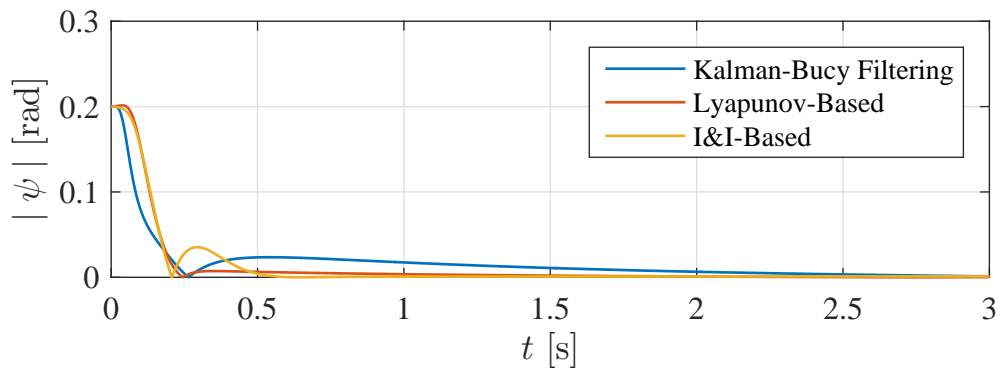
**Table 6.3:** Standard values of the parameters.

Figure 6.1 depicts the simulation with so called standard values of the parameters, which are shown in Table 6.3.

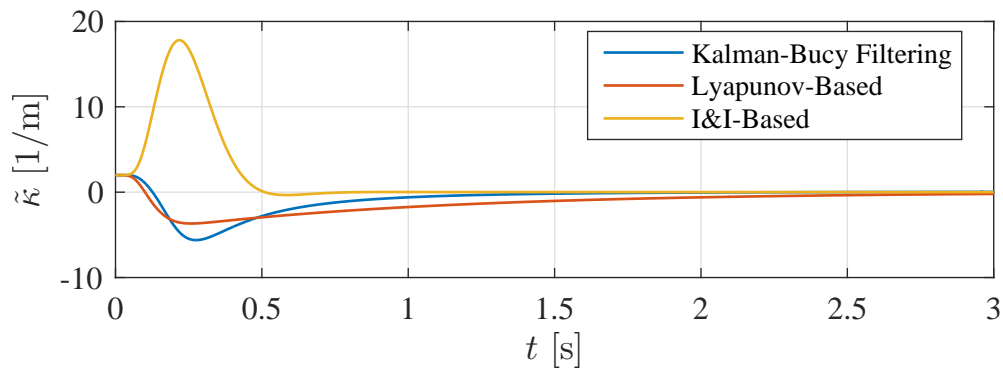
As shown in Figure 6.1, the simulation results of these standard scenario reveals that the estimated values with Kalman-Bucy Filtering, Lyapunov-based adaptive law and I&I converges to the actual values. However, every estimation method generates an overshoot of the estimated motion direction  $\hat{\mathbf{x}}_{\mathbf{h}}$ , which has the maximum for the Immersion and Invariance-based adaptive law at approximately 0.3s

$$\frac{\Delta|\psi|}{|\psi(\infty) - \psi(0)|} = \frac{|35 \cdot 10^{-3}|}{|0 - 0.2|} = 17.5\%, \quad (6.1)$$

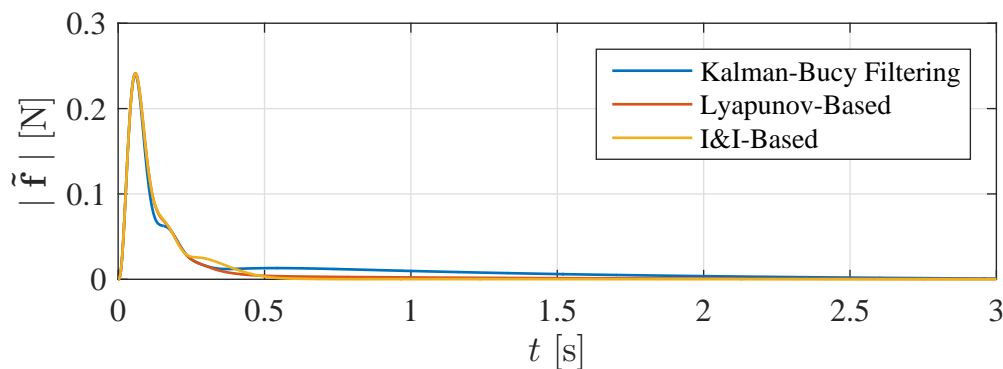
where  $\Delta|\psi|$  denotes the magnitude of the overshoot. Equation (6.1) shows that the relative overshoot is relatively large, however, the estimation of the motion direction with the Immersion and Invariance-based adaptive law has the best settling time, since the estimation error has the fastest convergence to zero. Furthermore, the I&I-based estimator shows the best performance regarding the parameter  $\hat{\kappa}$  and the state  $\hat{\mathbf{x}}_{\mathbf{h}}$  convergence. However, this estimator has the highest overshoot for the estimated inverse object length  $\hat{\kappa}$ , but this has no significant effect on the estimation of the motion direction  $\hat{\mathbf{x}}_{\mathbf{h}}$ .



(a) Estimation error response in the unconstrained direction.



(b) Estimated response for the inverse object length.

**Figure 6.1:** Estimation response of proposed estimators for the standard parameters, Table 6.3**Figure 6.2:** Simulated force error of the wrist mounted force sensor.

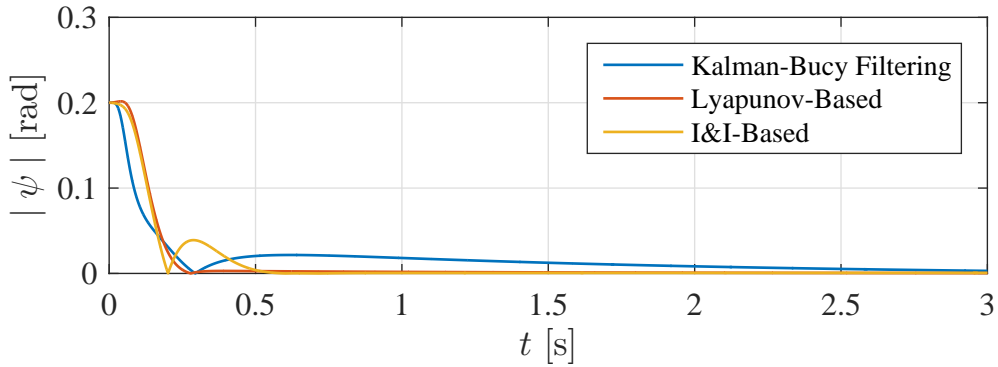
As depicted in Figure 6.2 the shapes of the sensor signals are similar, but the adaptive controller with Kalman-Bucy Filtering results to the slowest convergence to zero. The responses of the adaptive controller with Lyapunov-based and I&I-based adaptive laws are more or less the same.

### 6.1.1 Simulation Results for Varying Object Length

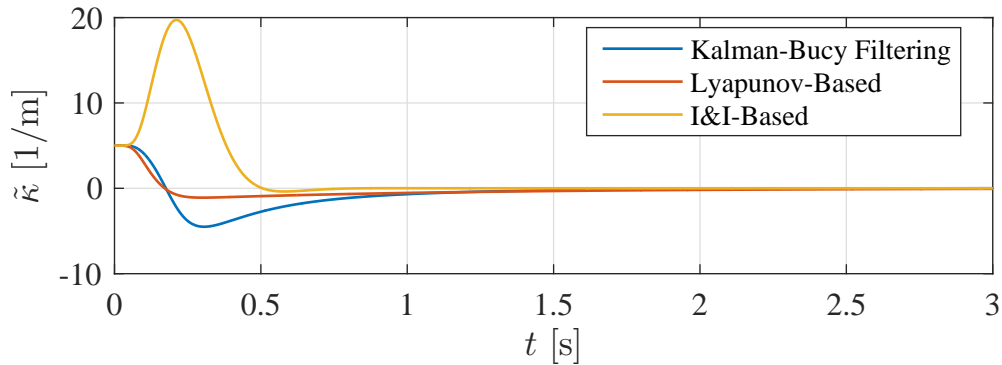
In order to test the robustness of the adaptive controller with the different estimation methods, the performance of the aforementioned three estimators are compared to each other. Only the parameter inverse object length of the plant is varying in this subsection. The controller and estimator parameters are the same. Table 6.4 shows the used simulation parameters for the following scenario.

Parameter	Value	Unit
$\kappa$	2	$\text{m}^{-1}$
$v_d^*$	0.05	$\frac{\text{m}}{\text{s}}$

**Table 6.4:** Values of the parameter with varying inverse object length simulation.



(a) Estimation error response in the unconstrained direction.



(b) Estimated response for the inverse object length.

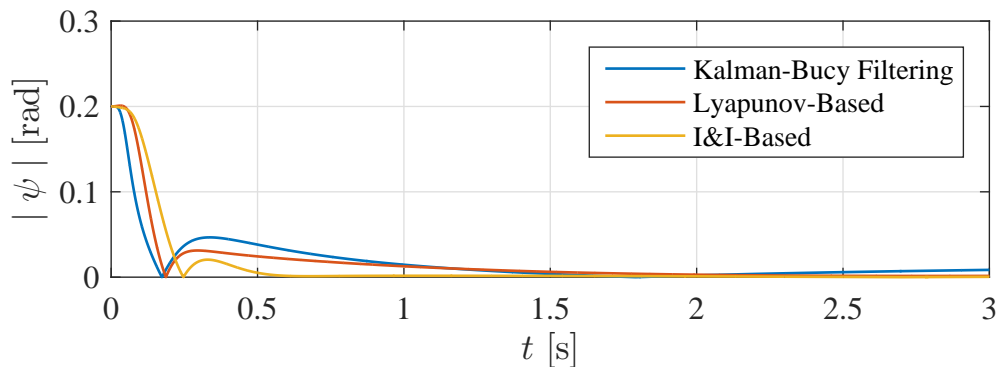
**Figure 6.3:** Estimation response of proposed estimators for inverse object length  $\kappa = 2\text{m}^{-1}$ .

Comparing the Figure 6.1a and 6.3a reveals that increasing the object length has no significant affect on the estimation performance of the motion direction. Only its settling time is slightly decreased. Changing of  $\kappa$  and keeping  $\hat{\kappa}(0)$  constant means that the initial estimation error is different for the object length varying scenarios. The convergence speed of  $\hat{\kappa}$  increases for the Lyapunov-based adaptive law and decreases for Kalman-Bucy Filtering in this scenario. The estimation performance

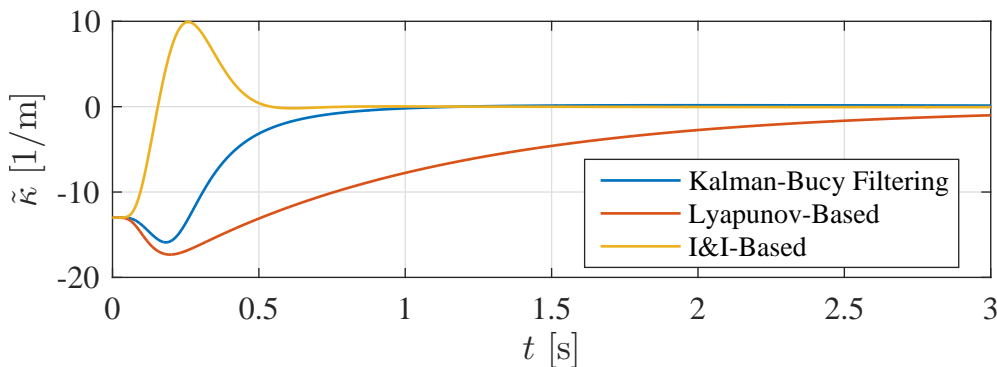
of the I&I-based adaptive law does not change. Table 6.5 shows the used simulation parameters for the following scenario.

Parameter	Value	Unit
$\kappa$	20	$\text{m}^{-1}$
$v_d^*$	0.05	$\frac{\text{m}}{\text{s}}$

**Table 6.5:** Values of the parameter with varying inverse object length simulation.



(a) Estimation error response in the unconstrained direction.

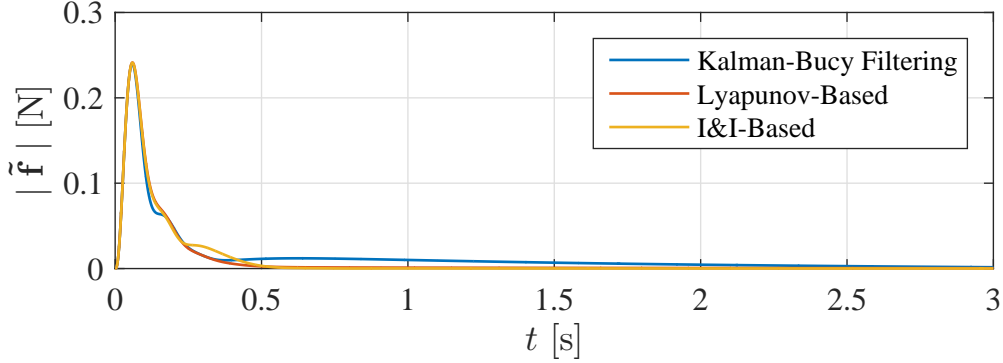


(b) Estimated response for the inverse object length.

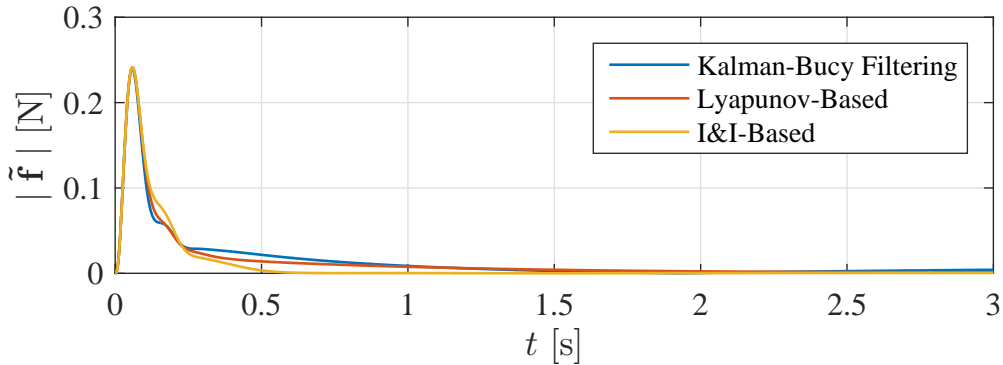
**Figure 6.4:** Estimation response of proposed estimators for inverse object length  $\kappa = 20\text{m}^{-1}$ .

Different object lengths imply different rotation velocities of the handle frame  $\{H\}$  for constant  $v_d$ . Figure 6.4a depicts that the overshoot for the unconstrained direction error increases for Kalman-Bucy Filtering and the Lyapunov-based adaptive law. This is caused by the increased estimation rate, since both estimations intersect the time-axis earlier compared to the standard value scenario. Comparing the Figures 6.1a, 6.3a and 6.4a reveals that estimation performance for the motion axis does not change significantly. Comparing the Figures 6.1b, 6.3b and 6.4b leads to the same statement for the estimation of the inverse object length, whereby the I&I-based adaptive law has the shortest settling time of the  $\kappa$  estimation. The varying object length scenarios shows that different  $\kappa$  and therefore different  $\tilde{\kappa}(0)$  has no significant effect on the estimation with Kalman-Bucy Filtering and I&I-based

adaptive law. In contrast, the settling time of the Lyapunov-based adaptive law depends on the object length in this case.



(a) Simulated error response of the force for the inverse object length  $\kappa = 2\text{m}^{-1}$ .



(b) Simulated error response of the force for the inverse object length  $\kappa = 20\text{m}^{-1}$ .

**Figure 6.5:** Estimation force error response of proposed estimators.

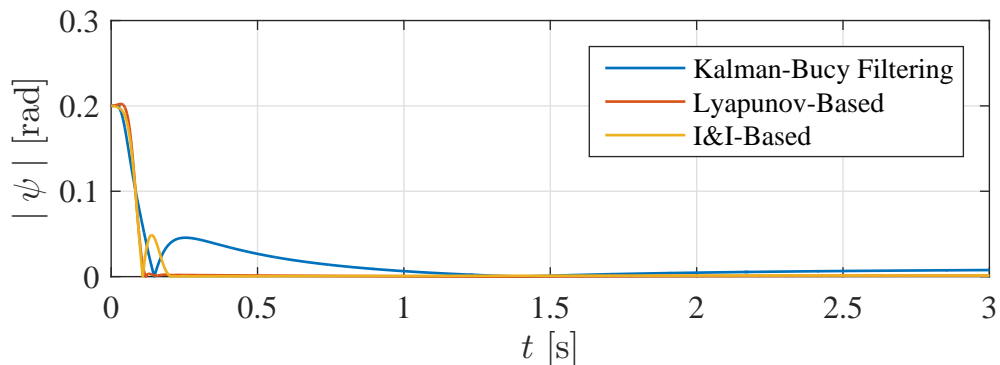
Figure 6.5a and 6.5b show that the occurring peak force is independent of the object length. Furthermore, the settling time of  $|\tilde{\mathbf{f}}|$  is affected by the object uncertainty of length, since the force error convergence for Kalman-Bucy Filtering and the Lyapunov-based adaptive is faster for short objects. The simulation results of this scenario indicate that the settling time for the I&I-based adaptive law is independent of the object length.

### 6.1.2 Simulation Results with Varying Desired Velocity

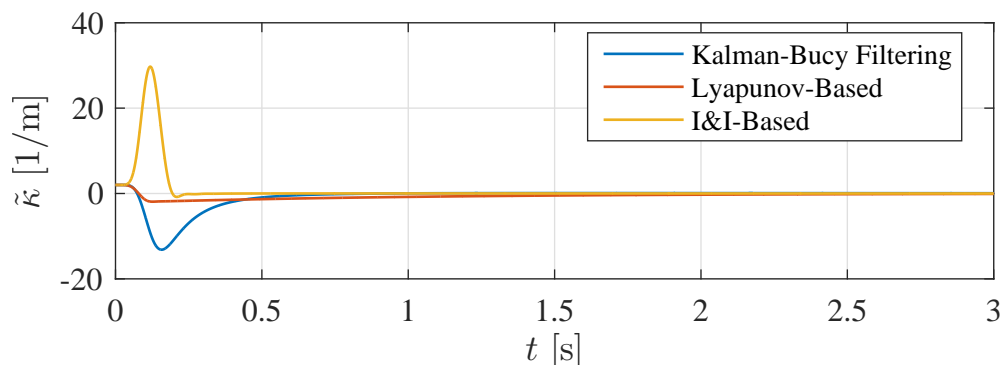
In this scenario, the desired velocity of the end-effector  $v_d$  is changing. Therefore, the rotation velocity of the handle frame  $\{H\}$  is higher compared to the standard value scenario. Table 6.6 shows the used simulation parameters for the following scenario.

Parameter	Value	Unit
$\kappa$	5	$\text{m}^{-1}$
$v_d^*$	0.1	$\frac{\text{m}}{\text{s}}$

**Table 6.6:** Values of the parameter with varying desired velocity.



(a) Estimation error response in the unconstrained direction.



(b) Estimated response for the inverse object length.

**Figure 6.6:** Estimation response of proposed estimators for desired velocity  $v_d^* = 0.1 \frac{\text{m}}{\text{s}}$ .

The higher velocity of end-effector significantly affects the settling time of the motion direction in all three estimator cases, which can be recognised in Figure 6.6a. In this case, the Lyapunov-based estimation has a negligible overshoot and the fastest settling time compared to the other estimators. The response of the object length is also different to the standard value scenario. First of all, the overshoot of the inverse object length estimation significantly increased for Kalman-Bucy Filtering and the I&I-based update law. Furthermore, the settling time of  $\hat{\kappa}$  decreased for all three estimators.

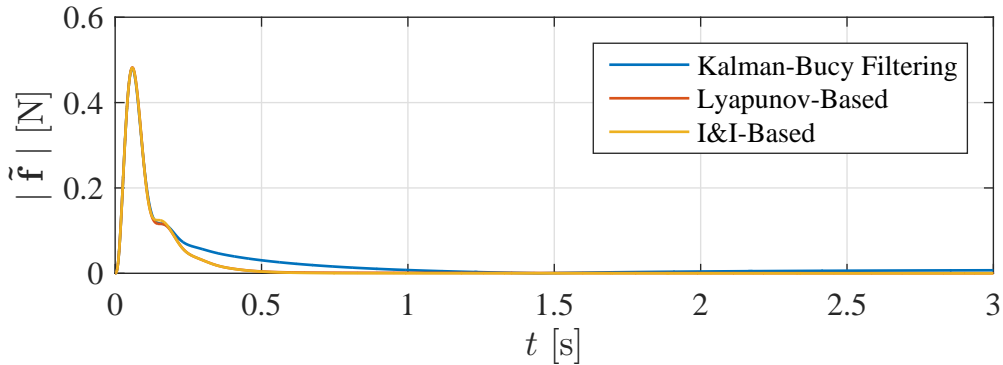


**Figure 6.7:** Estimation force error response of proposed estimators for the desired velocity  $v_d^* = 0.1 \frac{\text{m}}{\text{s}}$ .

A comparison of Figure 6.2 and 6.7 shows that the peak force increases for a higher desired velocity  $v_d^*$ . Additionally, the shape of the force error of the Lyapunov-based adaptive law and I&I adaptive law cannot be distinguished from each other. During this scenario,  $\tilde{\mathbf{f}}$  has a lower settling time as compared to the standard parameter scenario.

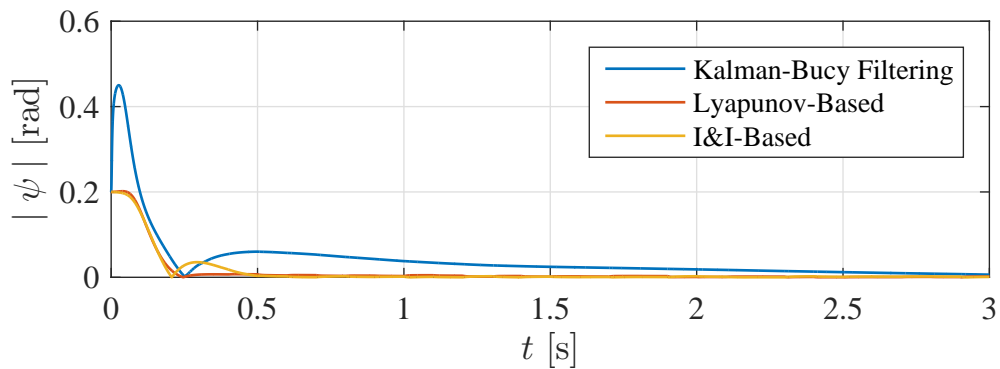
### 6.1.3 Simulation Results with Noise

In order to test the response of the adaptive controller with measurement noise, the force sensor signal  $\mathbf{f}$  is subjected to normally-distributed Gaussian noise with zero mean and the variance  $\sigma^2$ . Table 6.7 shows the used simulation parameters for the following scenario.

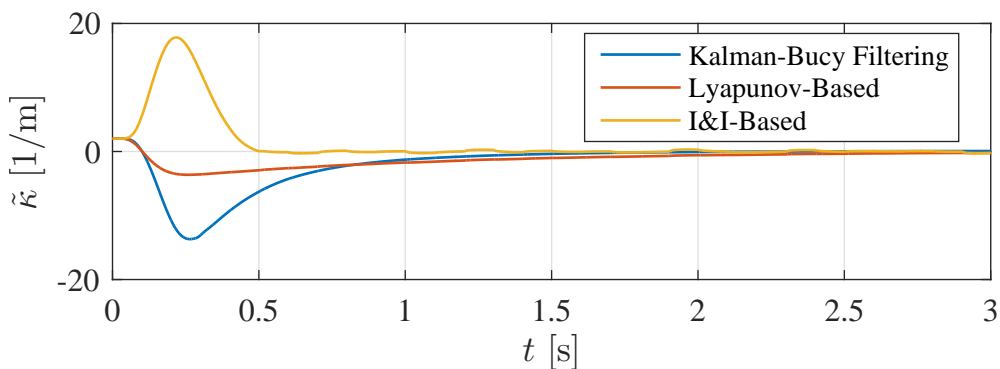
Parameter	Value	Unit
$\kappa$	5	$\text{m}^{-1}$
$v_d^*$	0.05	$\frac{\text{m}}{\text{s}}$
$\sigma^2$	$1 \cdot 10^{-6}$	N

**Table 6.7:** Values of the parameter with measurement signal noise.

As shown in Figure 6.8, the estimated motion direction and inverse object length converge to the actual values. Comparing the standard parameter and the noise scenario leads to the result that the performance of the Lyapunov-based and I&I-based adaptive controller does not change significantly. Only for the estimation values close to the actual values, the noise signal has a little influence on the estimation. In contrast, the estimation performance of Kalman-Bucy Filtering decreased for the noise subjected force signal  $\mathbf{f}$ . This could be seen clearly by comparing the peak value and the settling time of the error angle  $\psi$  in Figure 6.8 with Figure 6.1.



(a) Estimation error response in the unconstrained direction.



(b) Estimated response for the inverse object length.

**Figure 6.8:** Estimation response of proposed estimators for force measurement signal subjected to noise with variance  $\sigma^2 = 1 \cdot 10^{-6}$ N.

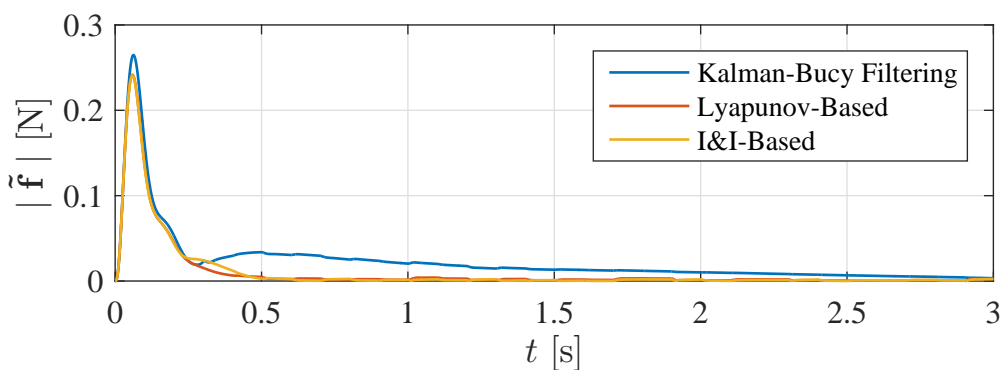


**Figure 6.9:** Estimation force error response of proposed estimators for force measurement signal subjected to noise with variance  $\sigma^2 = 1 \cdot 10^{-6}$ N.

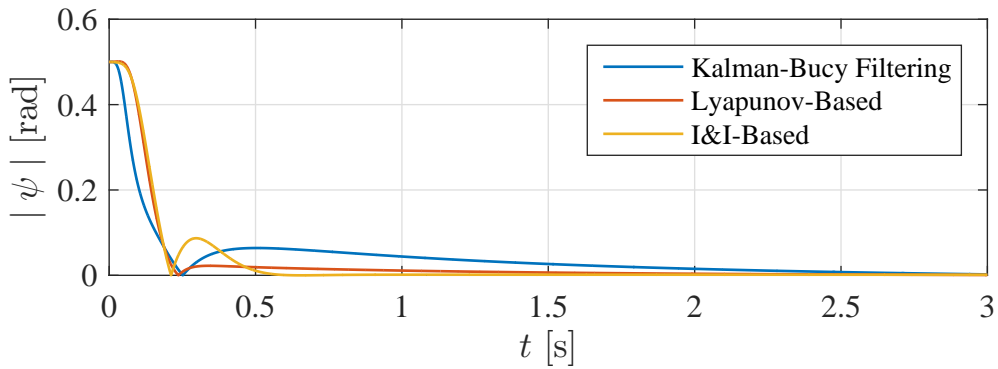
Figure 6.9 depicts that not only the peak of the error angle  $\psi$  but also the peak force increases. Furthermore, the peak force for the Kalman-Bucy Filter is higher than the adaptive controller using the adaptive laws. Additionally, the settling time for Kalman-Bucy Filtering is also higher compared to using the other estimators.

### 6.1.4 Simulation Results with Varying Initial Error Angle

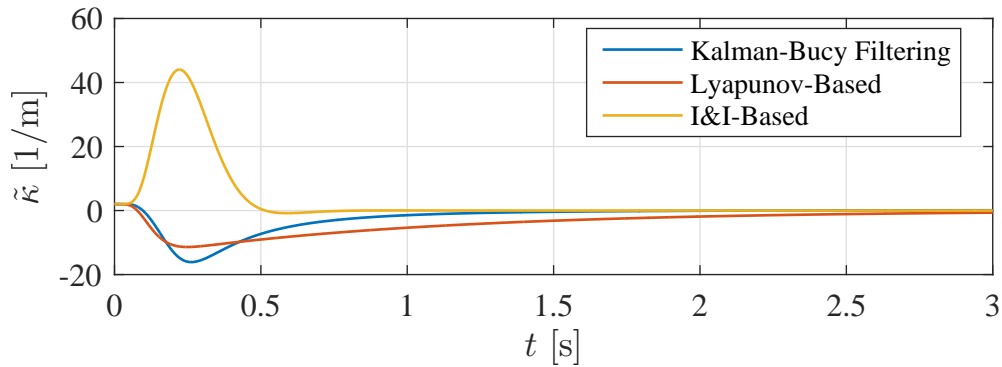
During this subsection, the initial value of the motion direction  $\hat{\mathbf{x}}_h(0)$  is changed, in order to evaluate the performance for different initial error angle  $\psi(0)$ . The adaptive controller in this scenario uses the standard parameters in Table 6.3. Additionally, the used initial values are presented in the following Table.

Parameter	Initial Value	Unit
$\hat{\kappa}(0)$	7	$\text{m}^{-1}$
$\psi(0)$	0.5	rad

**Table 6.8:** Initial estimates.



(a) Estimation error response in the unconstrained direction.



(b) Estimated response for the inverse object length.

**Figure 6.10:** Estimation response of proposed estimators for initial estimation error of the motion direction  $\psi(0) = 0.5\text{rad}$ .

Comparing Figure 6.1 and 6.10 indicates that the estimations possess the same shape, but due to the higher initial error of  $\psi$ , the course of the estimations are scaled up. That implies a higher peak and overshoot of the estimations.

The comparison of Figure 6.2 and 6.11 shows that the force error  $\tilde{\mathbf{f}}$  has the same convergence property as the aforementioned estimation error  $\psi$  and  $\tilde{\kappa}$ . It follows that a different initial motion direction offset  $\psi(0)$  has only influence on the peak and overshoot values. However, the settling time remains the same for this scenario.

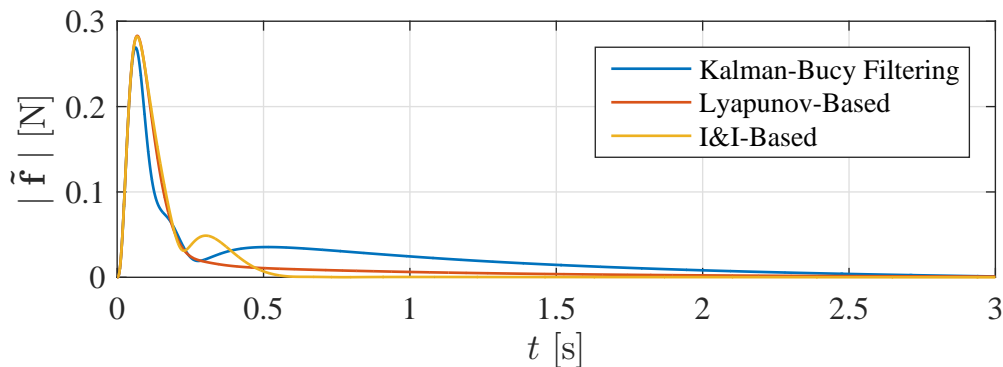


**Figure 6.11:** Estimation force error response of proposed estimators for initial estimation error of the motion direction  $\psi(0) = 0.5\text{rad}$ .

## 6.2 Discussion

The simulation results show that the Immersion and Invariance has the best performance for estimating the inverse length  $\kappa$  of the unknown object. However,  $\hat{\kappa}$  has a quite high overshoot all the simulated scenarios, which has no significant effect on the manipulation task. The reason is that the control law of the adaptive controller depends on the unknown motion direction of the object. The performance of I&I-based adaptive laws with respect to the estimation of the motion direction are comparable to the Lyapunov-based adaptive law. The latter one has often a smaller overshoot, but has a longer settle time. Additionally, both estimators have a sufficient high robustness against measurement noise. The simulated scenarios revealed that the Kalman-Bucy Filter has the worst performance for estimating the motion direction. Also, the simulation results show that the Kalman-Bucy Filter possesses a good performance in estimating the scaled rotation axis. Furthermore, the design method of the Kalman-Bucy Filter is quite simple compared to the other tested design methods.



# 7

## Conclusion

In this master thesis a generalised adaptive velocity controller was designed for manipulating objects with pivoting dynamics. The manipulation task consisted of rotating an unknown object around a pivot point on a supported surface. Additionally, the object was grasped in a way that allowed relative rotation between the end-effector and the object. To perform the manipulation task a velocity-controlled robot with a force/torque sensor was considered. The adaptive controller consisted of a control law using the force measurement signal and an on-line estimator for estimating the object posture and length. Kalman-Bucy Filtering, Lyapunov-based adaptive laws and I&I-based adaptive laws have been employed to solve this estimation problem.

Considering the results of the simulations in Chapter 6, the proposed adaptive controller with its three different estimators successfully estimates the unconstrained motion direction and the inverse object length on-line. Additionally, it is necessary to estimate the rotation axis of the object by Kalman-Bucy Filtering or the Lyapunov-based adaptive laws. Since the Immersion and Invariance framework uses a different parametrisation of the dynamical system, it is not necessary to solve the estimation problem for estimating the rotation axis. Also, the main condition  $\psi(0) \in \{\psi \in \mathbb{R} : |\frac{\pi}{2}|\}$  must be satisfied for every estimator to guarantee their performance.

In order to address possible extensions the following points could be added for further research on this field:

1. Position control
2. Virtual joint instead of physical joint

First of all, controlling the position of the unknown object could be interesting for door opening tasks, since a further manipulation task could consist of opening an unknown door, tracking the door opening angle and passing the door if the angle is large enough. The I&I-based estimator estimates the position of the object, since its design based on the alternative parametrisation (3.1) with known rotation axis. To take the estimation of the position for the other estimators into account, it is necessary to change their parametrisation.

Modelling a virtual joint instead of a physical joint could be another extension of the system. This means that the current revolute joint absorbs all forces, independent of their direction or magnitude. Regarding the direction, a virtual joint would absorb forces which have a positive normal force on the surface. However, for negative nor-

## 7. Conclusion

---

mal force virtual joint would not absorb the force and the object would lose contact with the surface. Another property of the virtual joint would be that it takes the friction into account. More precisely, the object will start sliding if the lateral force is high enough.

Additionally, in this master thesis the manipulation task of the object mainly consists of pivoting dynamics. In order to expand the applicability of an adaptive controller to more applications, it is possible to take friction and sliding effects into account instead of assuming a revolute joint.

# Bibliography

- [1] I. W. R. 2015, “IFR Press Conference.” [http://www.worldrobotics.org/uploads/tx\\_zeifr/Charts\\_PC\\_09\\_30\\_2015.pdf](http://www.worldrobotics.org/uploads/tx_zeifr/Charts_PC_09_30_2015.pdf), 2015. Accessed: 2016-01-19.
- [2] L. Sciavicco and B. Siciliano, *Modelling and Control of Robot Manipulators*. New York;London: Springer, 2000.
- [3] B. Siciliano and O. Khatib, *Springer Handbook of Robotics*. Berlin: Springer, 2008.
- [4] M. Vukobratovic, V. Potkonjak, and V. Matijevic, *Dynamics of Robots with Contact Tasks*, vol. 26. Dordrecht: Springer Netherlands, 2003.
- [5] A. De Luca and C. Manes, “Modeling of robots in contact with a dynamic environment,” *IEEE Transactions on Robotics and Automation*, vol. 10, no. 4, pp. 542–548, 1994.
- [6] V. F. Muñoz, J. M. Gómez-de Gabriel, I. García-Morales, J. Fernández-Lozano, and J. Morales, “Pivoting motion control for a laparoscopic assistant robot and human clinical trials,” *Advanced Robotics*, vol. 19, no. 6, pp. 694–712, 2005.
- [7] S. Erhart and S. Hirche, “Adaptive force/velocity control for multi-robot cooperative manipulation under uncertain kinematic parameters,” in *2013 IEEE/RSJ International Conference on Intelligent Robots and Systems*, pp. 307–314, Nov 2013.
- [8] Y. Karayiannidis, C. Smith, F. E. Vina, P. Ogren, and D. Kragic, “Model-free robot manipulation of doors and drawers by means of fixed-grasps,” pp. 4485–4492, IEEE, 2013.
- [9] Y. Karayiannidis, C. Smith, F. E. V. n. Barrientos, P. Ögren, and D. Kragic, “An Adaptive Control Approach for Opening Doors and Drawers Under Uncertainties,” *IEEE Transactions on Robotics*, vol. 32, pp. 161–175, Feb 2016.
- [10] D. E. Catlin, *Estimation, Control, and the Discrete Kalman Filter*, vol. 71. New York, NY: Springer New York, 1989.
- [11] M. S. Grewal, *Kalman Filtering: sTheory and Practice with MATLAB*. S.l.: Wiley-IEEE Press, 2015.
- [12] A. Astolfi, D. Karagiannis, and R. Ortega, *Nonlinear and adaptive control with applications*. London: Springer, 2008.
- [13] A. Astolfi and R. Ortega, “Immersion and invariance: a new tool for stabilization and adaptive control of nonlinear systems,” *IEEE Transactions on Automatic Control*, vol. 48, no. 4, pp. 590–606, 2003.
- [14] D. Karagiannis, R. Ortega, and A. Astolfi, *Nonlinear Adaptive Stabilization via System Immersion: Control Design and Applications*, vol. 311, pp. 1–21. London: Springer London, 2005.

- [15] I. N. Bronshtein, K. A. Semendyayev, G. Musiol, and H. Mühlig, *Handbook of Mathematics*. Berlin, Heidelberg: Springer Berlin Heidelberg, 6th 2015.;sixth; ed., 2015.
- [16] L. Råde and B. Westergren, *Mathematics Handbook for Science and Engineering*. Berlin, Heidelberg: Springer Berlin Heidelberg, fifth;5; ed., 2004.
- [17] P. Ioannou and J. Sun, *Robust Adaptive Control*. Prentice Hall PTR, 1995.
- [18] H. K. Khalil, *Nonlinear Systems*. Pearson, third;3 ed., 2001.
- [19] Y. Karayiannidis, C. Smith, F. Viña, P. Ögren, and D. Kragic, "Open Sesame!" Adaptive Force/Velocity Control for Opening Unknown Doors," *IEEE*, pp. 4040–4047, 2012.
- [20] The MathWorks, Inc., Natick, *SimMechanics Getting Started*, 4.8 ed., 2015.